# CARBON DIOXIDE ADSORPTION FROM REFINERY FLUE GASES

By

**Harsh Yadav**

**Roll No: 09MCH012**


**CHEMICAL ENGINEERING**

**(ENVIRONMENTAL PROCESS DESIGN)**

**AHMEDABAD-382481**

**May 2011**

# Carbon Dioxide Adsorption From Refinery Flue Gases

**Major Project**

Submitted in partial fulfillment of the requirements

For the degree of

Master of Technology in Chemical Engineering (Environmental Process Design)

By

**Harsh Yadav**

**Roll No: 09MCH012**


**DEPARTMENT OF CHEMICAL ENGINEERING**

**(ENVIRONMENTAL PROCESS DESIGN)**

**AHMEDABAD-382481**

**May 2011**

# Declaration

This is to certify that

i) The thesis comprises my original work towards the degree of Master of Technology in Chemical Engineering (Environmental Process Design) at Nirma University and has not been submitted elsewhere for a degree.

ii) Due acknowledgement has been made in the text to all other material used.

**Harsh Yadav**

# Certificate

This is to certify that the Major Project entitled ¨Carbon Dioxide Adsorption From Refinery Flue Gases ˝submitted by Harsh Yadav (09MCH012), towards the partial fulfillment of the requirements for the degree of Master of Technology in Chemical Engineering(Environmental Process Design) of Nirma University of Science and Technology, Ahmedabad is the record of work carried out by him under my supervision and guidance. In my opinion, the submitted work has reached a level required for being accepted for examination. The results embodied in this major project, to the best of my knowledge, haven't been submitted to any other university or institution for award of any degree or diploma.

Prof A.P Vyas
Guide,
Department of Chemical Engineering,
Institute of Technology,
Nirma University, Ahmedabad.

Dr. A.K Das , Dr. D Rajeshwar
Head of the Departement, A.V.P
Reliance Technology Group(RTG),
Reliance Industries Limited,
Jamnagar.

Dr. S.S Patel
Professor and HOD,
Department of Chemical Engineering,
Institute of Technology,
Nirma University, Ahmedabad.

Dr.K.Kotecha
Director,
Institute of Technology,
Nirma University, Ahmedabad.

# Abstract

Increasing awareness of the influence of greenhouse gases on global climate has led to recent efforts to develop strategies for the reduction of carbon dioxide ($CO_2$) emissions. Fossil-fueled power plants are responsible for roughly 40 percent of total $CO_2$ emissions, coal-fired plants being the main contributor. International Panel on Climate Change (IPCC) predicts that, by the year 2100, the atmosphere may contain up to 570 ppmv $CO_2$ against its present stage (389.91 ppmv), causing a rise of mean global temperature of around 0.9 °C and an increase in mean sea level of 0.38 m. In 2000, the burning of coal generated 37.8% of all $CO_2$ arising from fossil fuels [1] and as a result the strategy that is receiving the most attention involves the capture of $CO_2$ from large point sources (such as fossil fuel-fired power plants). In the history of civilizations, worldwide $CO_2$ emissions are increasing trend due to the rapid industrialization. The greenhouse gas can then be stored long term, either underground or in the ocean. However, to economically transport and store $CO_2$ it must be in a relatively pure high pressure form, requiring the separation and compression of $CO_2$ emitted by the power plant. The $CO_2$ capture step is projected to account for the majority of the expense for the overall carbon capture and subsequent storage process. There are three options to reduce $CO_2$ emissions into the atmosphere: To reduce energy intensity, to reduce carbon intensity, and to capture and store $CO_2$. The first two options require efficient usage of energy and a switch to non-fossil fuels such as hydrogen and renewable energy respectively. The third option requires the development of new efficient technologies for $CO_2$ capture and sequestration (CCS). The main application of $CO_2$ capture is likely to be at fossil fuel power plants, refineries, cement industries, which are contributing a large extent of $CO_2$ emissions into the atmosphere.

To date, all commercial $CO_2$ capture plants based on chemical absorption with an aqueous alkanolamine solvent of which monoethanolamine (MEA) is the most popular [2]. However, regarding their application to flue gases, these technologies need

significant modification to take care of high energy consumption and associated corrosion in presence of oxygen in flue gas. These ultimately lead to high capital and running costs. Therefore, although amine technology could be suitable for flue gases, the development of alternative low cost technologies could be crucial in the long term to provide a more cost and environmentally effective route to carbon capture and storage on a global scale. Adsorption is considered to be a promising technology for the efficient capture of $CO_2$ from flue gases.

To overcome the problems associated with current $CO_2$ capture techniques, this project involves the creation of a new generation of adsorbents - solids that can ¨soak up ¨$CO_2$ - to be used in power plants/ refinery. The adsorbents work on the principal that $CO_2$ is a weak acid that can be trapped onto a solid base with the right characteristics and well-developed pore-structure [3, 4]. Solid inorganic adsorbents will be created using support materials with numerous active sites to soak up $CO_2$. Adsorption capacities as a function of adsorbent properties, adsorbent loading, and flue gas compositions are described.

# Acknowledgements

I extend my sincere thanks to my guide Dr. A.K. DAS and Dr. D Rajeshwer,Reliance Technology Group (RTG), Jamnagar, for not only suggesting the research topic but also their invaluable guidance, keen interest, advice, and constructive criticism throughout the progress of project work.

I am also thankful to Dr. A.K. DAS, Head of the Department (HOD), Reliance Technology Group (RTG), Jamnagar, for giving me golden opportunity to gain such enriched knowledge at one of the leading research facility.

I am also thankful to my guide Professor A.P VYAS for his support and guidence through out the project work. He was a real source inspiration and encouragement through out the project duration.

I would like to express my immense and deep gratitude to Dr. N. Subramanyan,for his invaluable guidance throughout my project work. His unceasing dedication simulated me to accomplish my goal. He shaped my attitude toward research. I am feeling fortunate to be his student.

I take opportunity to express deep and sincere sense of gratitude towards Dr. S .S. Patel, Head of department, Department of Chemical Engineering, Institute of Technology, Nirma University, Ahmedabad. His constant help, thoughtful suggestions and kind co-operation have enabled me to complete this work.

I would like to thank Sukumar Mandal sir & Dr. Shrikant Dinda,Reliance Technology Group (RTG), Jamnagar, for their constant encouragement, kind co-operation, deep interest leading to progress of this project and creating a great piece of work atmosphere. I would like to place my respect and deep sense of gratitude to Surajit Sengupta sir, Ashwani sir, Anand, Arun D Arsu, Dr. Amit Deshmukh, Dr. G. Ravichandaran and Dr. Praveen Chinthala for their noble guidance and advice whenever I approached them.

I am thankful to Mrs. Sunita Parmar, Sumitra Maneria and M Manasa Reddy for their kind support and cooperation.

I also want to express my immense gratitude to my parents, sister, teachers and friends for their moral support to complete this work successfully. At last I express my sincere gratitude classmates.Finally I place my regards to all those who helped me knowingly or unknowingly.

At last but not the least I also want to thank the almighty god for helping me in completing the work.

**Harsh Yadav**

**09MCH012**

# Contents

# List of Tables

# List of Figures

# Chapter 1

# Introduction

Reducing carbon dioxide ($CO_2$) emissions for addressing climate change concerns is becoming increasingly important as the $CO_2$ concentration in the atmosphere has increased rapidly since the industrial revolution. Many mitigation methods, including $CO_2$ sequestration and utilization, are currently being explored and require $CO_2$ in a concentrated form ($>$ 95 vol %). However the $CO_2$ from large sources, such as flue gases from fossil fueled power plants and refineries is available in dilute form with impurities. Therefore, capturing $CO_2$ from flue gas is an important common link for many mitigation methods

Increasing awareness of the influence of greenhouse gases on global climate has led to recent efforts to develop strategies for the reduction of carbon dioxide ($CO_2$) emissions. Fossil-fueled power plants are responsible for roughly 40 percent of total $CO_2$ emissions [1], among them coal-fired power plants being the main contributors. Intergovernmental Panel on Climate Change (IPCC) predicts that, by the year 2100, the atmosphere may contain up to 570 ppmv $CO_2$ [1] against its present stage (389.91 ppmv), causing a rise of mean global temperature of around 0.9 °C and an increase in mean sea level of 0.38 m. In 2000, the burning of coal generated 37.8% of all $CO_2$ arising from fossil fuels [2]. As a result, it is important to capture $CO_2$ from large point sources, such as fossil fuel-fired power plants. In the history of civilizations, worldwide $CO_2$ emissions show an increasing trend due to the rapid industrialization

with contribution of different industries.

Current technologies being considered for $CO_2$ sequestration include: disposal of $CO_2$ in deep oceans; depleted oil and gas fields; deep saline formations (aquifers); and recovery of enhanced oil, gas and coal-bed methane. However, the current cost for the utilization of such technologies is found to be too expensive. The cost of separation and capture, including compression to the required pressure for the sequestration step are generally estimated to comprise about three-fourths of the total cost of ocean or geologic sequestration. An improvement of the separation and capture of $CO_2$ will reduce the total cost required for sequestration [3].

The $CO_2$ capture step is projected to account for the majority of the expense for the overall carbon capture and subsequent storage process. There are three options to reduce $CO_2$ emissions into the atmosphere: a) to reduce energy consumption b) to reduce carbon consumption of fuel c) to capture and store $CO_2$. The first two options require efficient usage of energy and a switch to non-fossil fuels such as hydrogen and renewable energy respectively. The third option requires the development of new efficient technologies for $CO_2$ capture and sequestration (CCS). The main application of the post-combustion $CO_2$ capture is likely to be at fossil fuel power plants, refineries, cement industries, which contribute to a large extent of $CO_2$ emissions into the atmosphere. A comparison of various post-combustion $CO_2$ capture routes are described in the Table 1.1 . To date of all commercial $CO_2$ capture plants, chemical absorption with an aqueous alkanolamine solvent of which monoethanolamine (MEA) is the most popular [4]. However, regarding their application to flue gases, these technologies need significant modification to take care of high energy consumption and associated corrosion in presence of oxygen in flue gas. These ultimately lead to high capital and running costs. Therefore, although amine technology could be suitable for flue gases, the development of alternative low cost technologies could be crucial in the long term to provide a more cost and environmentally effective route to carbon capture and storage on a global scale. Adsorption is considered to be a promising technology for the efficient capture of $CO_2$ from flue gases. The present

Table 1.1: Comparison of Various Post-combustion $CO_2$ Capture Processes

| Process | Energy consumption | Cost of capture | Merits | Demerits |
|---|---|---|---|---|
| Absorption Process (Amine) | 1.0 Mcal/kg$CO_2$ $\Delta\ H_{abs} = -1300$ kcal/kg$CO_2$ | 40 to 60 US$/Ton of $CO_2$ | 90% removal Bulk Handling | Degradation of adsorbent, Large energy consumption, Corrosion Problem |
| Adsorption Process (Alkali promoted) | 0.669 Mcal/kg$CO_2$ $\Delta\ H_{ads} = -630$ kcal/kg$CO_2$ | 17 to 25 US$/Ton of $CO_2$ | 90% removal Lower Energy and cost | Limit of adsorbents,Relatively complex configuration |
| Membrane Process | 0.597 Mcal/kg$CO_2$ | 200 US$/Ton of $CO_2$ | 80% removal Lower Energy | Aging of membrane,High pressure operation and cost |

study focuses on carbon dioxide removal by adsorption process using sodium carbonate impregnated on support as an adsorbent. The adsorption process has lower heat demand since it operates at lower $\Delta$ T between adsorption/ desorption. The heat of adsorption is also much lower ($\sim$50%) than the amine absorption process.

None of the currently available $CO_2$ capture processes are economically feasible on an implementation scale to capture $CO_2$ for sequestration, since they consume large amounts of parasitic power and significantly increase the cost of electricity. The costs of separation and capture, including compression to the required pressure for the sequestration step are generally estimated to comprise about three-fourths of the total cost of ocean or geologic sequestration. An improvement of the separation and capture of $CO_2$ will reduce the total cost required for sequestration.

The goal of $CO_2$ separation and capture is to recover $CO_2$ from its many sources in a form suitable for transport and sequestration. The most likely options for $CO_2$ separation and capture include chemical absorption, physical and chemical adsorption, low-

temperature distillation, gas-separation membranes, mineralization/bio-mineralization, and vegetation. The most commonly used method today is absorption of carbon dioxide by chemical or physical solvents. For low $CO_2$ concentrations the chemical solvents such as alkanolamines are used. For higher partial pressures physical absorbents like cold methanol, propylene carbonate, etc are preferred. But these processes have many disadvantage like energy intensive, low capacity ($CO_2$ absorbed per unit mass), amine solution also has a limited lifetime due to degradation through oxidation of the amine. In addition, corrosion problems are usually observed for the aqueous amine process. Recently, several solids sorbents have been utilized to remove carbon dioxide from enclosed environments such as submarines, aircrafts, spacecrafts, and enclosed pressurized chambers. Porous materials, like activated carbons and zeolites, are suitable candidates for $CO_2$ capture by physical adsorption, due to their highly developed porous structure. The other adsorbents which can be considered are Hydrotalcites, Carbon fiber composite molecular sieves, Metal oxides, and Metal organic frameworks.

Thus, improved $CO_2$ capture technologies are vital if the promise of geologic sequestration, enhance oil recovery (EOR), and enhanced coal bed methane (ECBM) production is to be realized.

The present study focuses on carbon dioxide removal by adsorption process using sodium carbonate impregnated on support as an adsorbent. The main objectives of the present study are:

- Synthesis and preparation of adsorbents (sodium carbonate and other inorganic/ organic materials) with specific pore structures and surface areas.
- Characterization and analysis of synthesized adsorbents for their relevant properties.
- Investigation on the kinetics of $CO_2$ removal using different adsorbents from refinery flue gas streams.

- Fitting the experimentally obtained isotherms in appropriate available models and to studying heat of adsorption and selectivity for removal $CO_2$ from flue gases.

## 1.1 Objective of the Work

The objective of this work is to develop adsorbent with specific pore structures and surface areas for adsorption of $CO_2$ from refinery flue gases.

## 1.2 Scope of the Work

Characterization and analysis of synthesized adsorbents for their relevant properties.Investigation of the adsorption capacity of $CO_2$ using different adsorbents from refinery flue gas streams.And fitting the experimental data into models.

## 1.3 Thesis Organization

The rest of the thesis is organized as follows.

**Chapter 2**, *Literature Survey*, Describe the carbon dioxide emissions and environmental problems related with it. It describes different mitigation techniques. Also gives the different approaches used to capture carbon dioxide. It also discuss the phenomenon of adsorption

**Chapter 3**, *Experimental Methods*, It gives detail about the materials used for preparation of adsorbent and the method of preparation of adsorbents.This chapter describe the experimental set up. Also gives the Design of Experiment(DOE)that was followed during the study and the reaction chemistry of the experiment and also discuss about the various models that are being used for the study

In **chapter 4**, *Results and discussion*, The Experimental Results are discussed in this chapter.

Finally, in **chapter 5**,*Conclusion*, The conclusion is drawn and forward path is also given

# Chapter 2

# Literature Survey

## 2.1 Carbon dioxide emissions and Environmental problems

### 2.1.1 Carbon dioxide and greenhouse effect:

One of the most alarming global environmental problems of today, is the projected increase of the natural greenhouse effect resulting from increased production of greenhouse gases. Over the last two decade, considerable increase in the accumulation of greenhouse gases in the atmosphere has been observed, the most important of which is carbon dioxide, and its associated role in causing global climate warming. Global warming is a process in which the surface temperature of the Earth rises because of the "greenhouse effect". According to the National Academy of Sciences, the Earth's surface temperature has risen by about 1°C in the past century, with accelerated warming during the past two decades. There is new and stronger evidence that most of the warming over the last 50 years is attributable to human activities. Human activities have altered the chemical composition of the atmosphere through the build up of greenhouse gases - primarily carbon dioxide, methane, and nitrous oxide. If things continue the way they are, in another 100 years the average temperature will

be about 2°C higher than it is today.[7]

Amongst all greenhouse gases, $CO_2$ receives the most attention. Although the radiative forcing of $CO_2$ is much less than other greenhouse gases ($CH_4$, $N_2O$, CFCs, etc.), $CO_2$ is emitted in large amounts into the atmosphere and has a rather long atmospheric lifetime. Greenhouse gases in the decreasing order of radiative forcing are CFCs (0.07w/$m^2$)>$N_2O$ (0.15w/$m^2$)>$CH_4$ (0.48w/$m^2$)>$CO_2$ (1.46w/$m^2$). When all these parameters are modelled, to evaluate the global warming potential, $CO_2$ is estimated to contribute approximately 60% of the enhanced greenhouse gas effect. The other greenhouse gases such as methane accounts for about 20% nitrous oxide accounts for about 5% and CFCs accounts for about 15% of the greenhouse effect.[8]

### 2.1.2 Effect of global warming:

The potential major effects of global warming include: [8, 9]

- **In the land:** The water cycle of evaporation and precipitation is predicted to grow more agitated, destroying the current balance of water resources. This will result in some areas suffering from frequent flooding while others suffer from drought.

- **In the air:** Changes in the temperature structure of the atmosphere (the troposphere and stratosphere) are expected to exert complex effects on the ozone layer and increase the likelihood of photochemical smog.

- **In the ocean:** As the temperature of the seas and oceans rises, their volume will increase, melting glaciers and other frozen storehouses of water. This will cause sea levels to rise to an expected 15 to 95cm higher than they are today, by 2100. And the seas will continue rising, submerging vast expanses of beach and making some countries lose their land.

- It could also affect human health, animals, and many types of ecosystems. Deserts may expand into existing rangelands, and features of some of our Na-

tional Parks may be permanently altered. Changing regional climate could alter forests, crop yields, and water supplies.

### 2.1.3 Carbon dioxide emissions:

The exponential growth of the global economy since 1860 has been based on fossil fuel consumption. During this period, mankind has collectively released approximately 950 billion tons of carbon dioxide (260 Gtons of carbon) from the burning of oil, coal and natural gas. These fossil fuel emissions have been increasing at an average rate of 2% a year to a 1997 annual global output of around 23 billion tons of carbon dioxide (6.3 Gtons of carbon). Roughly half of these emissions (3.5 Gtons of carbon) remain in the atmosphere, the rest being adsorbed by natural processes. $CO_2$ concentrations have increased by 35% from the pre-industrial 280 ppmv to the current level of around 390 ppmv. [10]

$CO_2$ emissions from refineries account for about 4% of the global $CO_2$ emissions, close to 1 billion tons of $CO_2$ per year[11]. The $CO_2$ emissions from refineries form a very substantial part of the overall group $CO_2$ emissions. One of the routes to reduce refinery emissions is via carbon capture and storage.

Table 2.1: Global stationary CO2 emitters.Emissions from transportation sector not included (IPCC, 2005)

| Process | Number of Sources | Emissions (Mt$CO_2$/ Yr) |
|---|---|---|
| Power | 4942 | 10539 |
| Cement Production | 1175 | 932 |
| Refineries | 638 | 798 |
| Iron and Steel Industry | 269 | 646 |
| Petrochemical Industry | 470 | 379 |
| Oil and Gas Processing | N\A | 50 |
| Other sources | 90 | 33 |
| Bioethanol and Bioenergy | 303 | 91 |
| Total | 7887 | 13466 |

Globally, the refining sector ranks third among stationary $CO_2$ producers, after the

power production sector and the cement industry. Other large producers are the iron and steel industry, and the petrochemicals industry Table 2.1 [11]. Together, stationary sources amount to about 60% of overall global $CO_2$ emissions.

$CO_2$ may be emitted at refineries from a variety of sources. For a typical complex

Table 2.2: Overview of major CO2 emission sources in a typical complex refinery

| $CO_2$Emitter | Description |
|---|---|
| Furnace and Boiler | Heat required for the separation of the liquid feed and to provide heat of reaction to refinery processes such as reforming and cracking. |
| Utilities | $CO_2$ from the production of electricity and steam at a refinery. |
| Fluid Catalytic Cracker | Process used to upgrade a low hydrogen feed to more valuable products. |
| Hydrogen Manufacturing | For numerous processes, refineries require hydrogen. Most refineries produce this hydrogen on site. |

refinery, the key sources of $CO_2$ are presented in Table 2.2 [11].

Increasing awareness of the influence of greenhouse gases on global climate has led to recent efforts to develop strategies for the reduction of carbon dioxide ($CO_2$) emissions. In 2000, the burning of coal generated 37.8% of all $CO_2$ arising from fossil fuels [11] and as a result the strategy that is receiving the most attention involves the capture of $CO_2$ from large point sources. The greenhouse can then be stored long term, either underground or in the ocean. However, to economically transport and store $CO_2$ it must be in a relatively pure high pressure form, requiring the separation and compression of $CO_2$ emitted by the stationary source.

### 2.1.4 Carbon sequestration:

Carbon sequestration refers to the provision of long-term storage of carbon in the terrestrial biosphere, underground, or the oceans so that the build-up of carbon dioxide concentration in the atmosphere will reduce or slowdown.[12] There are many options available for $CO_2$ sequestration, some of which are discussed as follows:

**Geologic Sequestration** :

Carbon dioxide sequestration in geologic formations includes oil and gas reservoirs, unmineable coal seams, and deep saline reservoirs. These are structures that have stored crude oil, natural gas, brine and $CO_2$ over millions of years. In many cases, injection of $CO_2$ into a geologic formation can enhance the recovery of hydrocarbons, providing value-added byproducts that can offset the cost of $CO_2$ capture and sequestration. Some of the methods for geologic sequestration $CO_2$ are given below:

- Oil and Gas Reservoirs: In some cases, production from an oil or natural gas reservoir can be enhanced by pumping $CO_2$ gas into the reservoir to push out the product, which is called enhanced oil recovery.

- Coal Bed Methane: Coal beds typically contain large amounts of methane-rich gas that is adsorbed onto the surface of the coal. The current practice for recovering coal bed methane is to depressurize the bed, usually by pumping water out of the reservoir. An alternative approach is to inject carbon dioxide gas into the bed. Tests have shown that the adsorption rate for $CO_2$ to be approximately twice that of methane, giving it the potential to efficiently displace methane and remain sequestered in the bed.

- Saline Formations: Sequestration of $CO_2$ in deep saline formations does not produce value-added by-products, but it has other advantages such as large storage capacity and easy access to a saline formation injection point.[12, 13, 14]

**Ocean Sequestration**:

$CO_2$ is soluble in ocean water, and through natural processes the oceans both absorb and emit huge amounts of $CO_2$ into the atmosphere. It is widely believed that the oceans will eventually absorb 80-90 percent of the $CO_2$ in the atmosphere and transfer it to the deep ocean. However, the kinetics of ocean uptake are unacceptably slow.

**Terrestrial Sequestration**:

Vegetation and soils are widely recognized as carbon storage sinks. The global biosphere absorbs roughly 2 billion tons of carbon annually, an amount equal to roughly

one third of all global carbon emissions from human activity. Significant amounts of this carbon remains stored in the roots of certain plants and in the soil. In fact, the inventory of carbon stored in the global ecosystem equals roughly 1,000 years worth of annual absorption, or 2 trillion tons of carbon. Terrestrial carbon sequestration is defined as either the net removal of $CO_2$ from the atmosphere or the prevention of $CO_2$ net emissions from the terrestrial ecosystems into the atmosphere.

## 2.2 Different methods for carbon dioxide removal:

Removal of carbon dioxide from gas streams is already in use for some industrial purposes such as chemical synthesis and purification of natural gas. A wide range of techniques is being developed to remove the carbon dioxide from flue gases generated due to fossil fuels combustion before it is released to the atmosphere. These can be divided into three main types:

- Pre-combustion capture
- Post-combustion capture
- Oxy fuel combustion

### 2.2.1 Pre-combustion capture:

It is the removal of the carbon dioxide before the fuel is used for energy production. The fossil fuel is treated to allow $CO_2$ to be separated, leaving a hydrogen-rich fuel. The current method in use is by reforming natural gas with steam, to produce $CO_2$ and hydrogen. The fuel is reacted with oxygen or air, and in some cases steam, to give mainly carbon monoxide and hydrogen. The carbon monoxide is reacted with steam in a catalytic reactor, called a shift converter, to give $CO_2$ and more hydrogen. The $CO_2$ is separated and the hydrogen is used as fuel in a gas turbine combined cycle plant. The process is, in principle, the same for coal, oil or natural gas, but when coal

or oil are used there are more stages of gas purification, to remove particles of ash, sulphur compounds and other minor impurities[15]. Figure 2.1 shows a simplified diagram of a coal fired power plant with pre-combustion capture of $CO_2$.

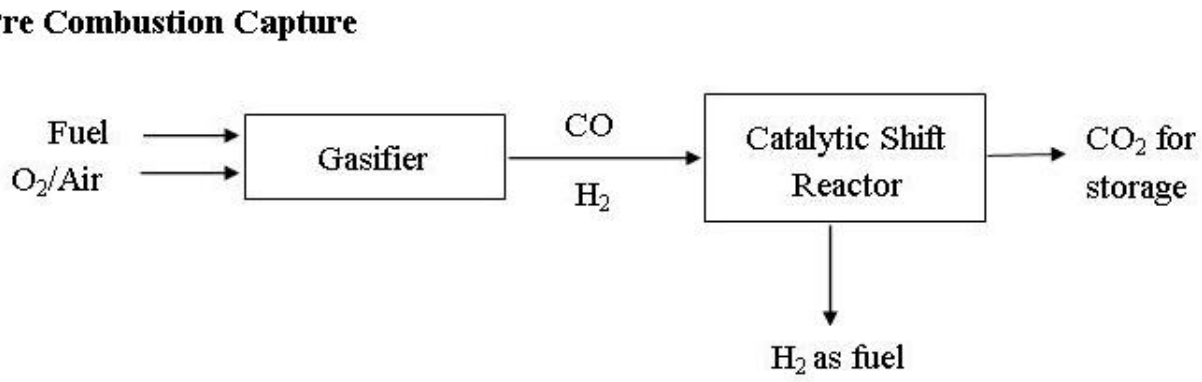


Figure 2.1: Pre-combustion capture of $CO_2$

There are three reasons for finding a pre-combustion approach more attractive than post-combustion [16]:

- It uses natural gas reforming technique which is deployed on a huge scale in chemical industries. Gasification of coal relies on Integrated Gasification Combined Cycle (IGCC) power plants. These are not yet commercial, but the technology has been developed and demonstrated; IGCC plants have long been advocated for their relatively high efficiency and low levels of conventional pollutants.

- They yield much higher concentrations of $CO_2$ than are present in conventional flue gases, and at higher pressure. So the volume of gas being treated is lower, thus reduces capital cost; and the higher concentration of $CO_2$ means that less powerful solvents are needed, this makes the capture of the $CO_2$ more energy efficient and thus potentially cheaper.

- The hydrogen produced could alternatively be used to generate electricity in a

fuel cell.

It is possible to retrofit many existing coal and gas fired generators for $CO_2$ capture but these techniques are very expensive requiring high capital investment which have kept them from being commercially viable.

### 2.2.2 Oxy fuel Combustion Approach:

Air fed to the combustion chamber has only around 20% oxygen in normal conditions, with most of the rest being nitrogen, which is largely inert. By increasing the proportion of $O_2$ a more efficient and complete combustion can be achieved. An advantage of this approach is that it results in much higher concentrations - between 55 and 60% - of $CO_2$ in the flue gases. If the flue gas is recycled into the combustion chamber and a relatively pure $O_2$ feed is used, flue gas $CO_2$ can be as high as 90%Ṫhe disadvantage of oxy fuel combustion is that a large quantity of oxygen is required, which is expensive, both in terms of capital cost and energy consumption.[15, 17]A simplified diagram of oxy fuel combustion approach is shown in Figure 2.2 .

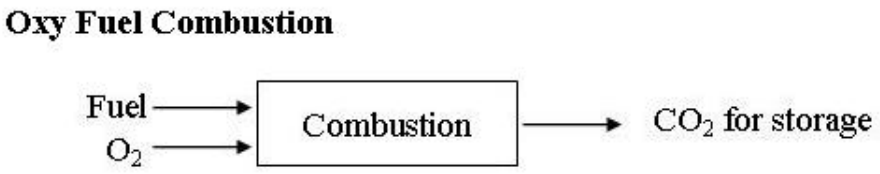


Figure 2.2: Oxy fuel combustion capture of $CO_2$

### 2.2.3 Post-combustion capture:

It involves the extraction of carbon dioxide from the flue gases ejected after combustion of the fossil fuels. Figure 2.3 shows a simplified diagram of a post-combustion capture of $CO_2$. There are many techniques available to separate $CO_2$ from flue gases. The preferred option depends in large part on the concentration of $CO_2$ in the gas stream.

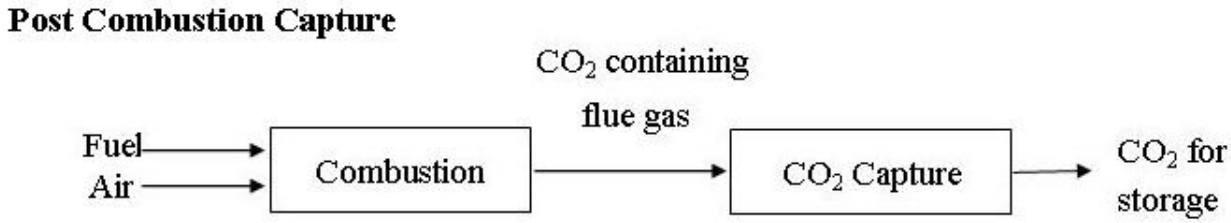


Figure 2.3: Post- combustion capture of $CO_2$

**Chemical absorption**:

The $CO_2$ absorption process using aqueous amine solutions has been extensively used for the removal of $CO_2$ from gas streams in many industries. This process based on the principles of chemical absorption of $CO_2$ via monoethanolamine (MEA), diethanolamine (DEA), or methyldiethanolamine (MDEA) is considered to be a potential technique for capturing greenhouse gas emission from flue gas streams. Wet chemical stripping of $CO_2$ involves one or more reversible chemical reactions between $CO_2$ and another material such as MEA to produce a liquid species which, upon heating, breaks down to liberate $CO_2$, and regenerate the original material used to react with $CO_2$. The chemical reaction between MEA and $CO_2$ is[17]:

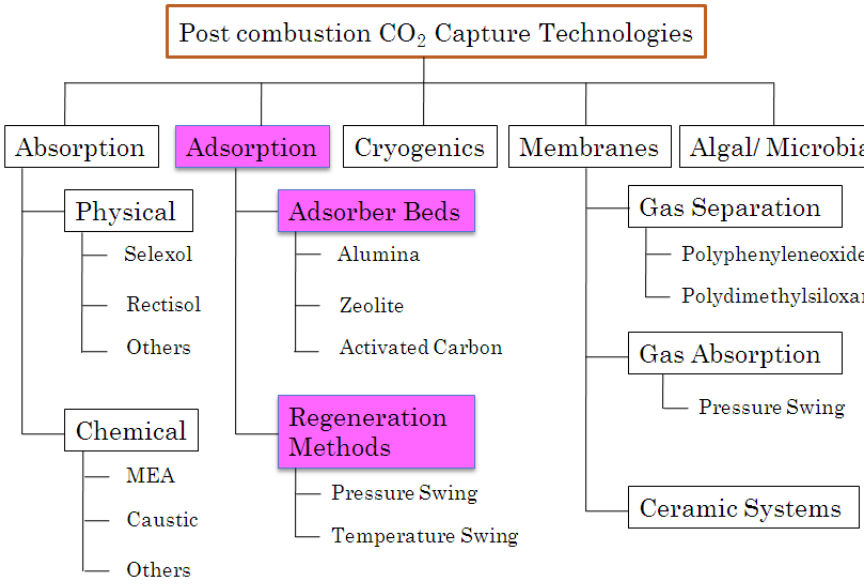


Figure 2.4: Different routes for Post- combustion capture of $CO_2$

$$C_2H_4OHNH_2 + CO_2 + H_2O \rightarrow C_2H_4OHNH_3 + HCO_3$$

Limitations of Amine-based Processes are:[15, 18, 19]

- $CO_2$ is absorbed much more easily into solvents at high pressure but the flue gases from the power plants are emitted at low pressure.
- The energy intensity processes due to their low capacity ($CO_2$ absorbed per unit mass). Therefore, a large volume of liquid is required to release a small amount of gas.
- Amine solution also has a limited lifetime due to degradation through oxidation of the amine. Oxygen present in the gas stream oxidizes the amine particularly during desorption when the sorbent is heated.
- Sulfur oxides ($SO_2$, $SO_3$) react with MEA to form heat-stable corrosive salts that cannot be reclaimed.

- Nitrogen oxides ($NO_2$, NO) are also present in the flue gas. The main component NO is relatively inert gas but $NO_2$ will partially lead to form heat stable salt.

- Fly ash in the flue gas can cause foaming and degradation of the solvent and plugging and scaling of the process equipment.

- Flue gas entering the absorber at high temperatures can lead to solvent degradation and decreased absorption efficiency.

- The process requires extensive equipment for circulating large volumes of liquid absorbents and for heat exchange.

For higher partial pressures of carbon dioxide in flue gas physical absorbents are preferred. These include cold methanol and propylene carbonate. Calcium oxide (which produces limestone when combined with $CO_2$), sodium hydroxide and potassium hydroxide are also viable absorbers. Use of aqueous potassium carbonate systems promoted by secondary amines is another option for high partial pressure gases but the process involves high heat of absorption.[20, 21]

Recently, other solvents such as ammonia, mixed amines (aqueous blends of methyl-diethanolamine (MDEA) and monoethanolamine (MEA), as well as 2-amino-2-methyl-1-propanol (AMP) and monoethanolamine (MEA) have also been tested [22].Carbon dioxide removal efficiencies in the range from 95% to 99% can be achieved by means of ammonia scrubbing [23]. Also absorption capacity and absorption rates are higher than MEA process. The energy requirement for the regeneration of $NH_3$ reagent is less than that for the regeneration of MEA reagent [24].

**Physical adsorption**:

An adsorption process consists of two major steps: adsorption and desorption. The technical feasibility of a process is dictated by the adsorption step, whereas the desorption step controls its economic viability. Strong affinity of an adsorbent for removing the carbon dioxide from a flue gases is essential for an effective adsorption step. The

stronger the affinity, however, the more difficult it is to desorb the gas impurity and the higher the energy consumed in regenerating the adsorbent for reuse in the next cycle. The desorption step, therefore, has to be very carefully balanced against the adsorption step for an adsorption step to be successful.[18, 19]

The main advantage of physical adsorption over chemical or physical absorption is its simple and energy efficient operation and regeneration, which can be achieved with a pressure swing or temperature swing cycle. Typical substances for this use include Zeolites, activated carbon, metal oxide sorbent and hydrotalcite like compounds.

**Gas membranes**:

A membrane is a film that allows selective permeation of different gases under specific conditions. These are divided into gas separation membranes and gas absorption membranes. The first of these is a thin film of a ceramic or polymeric material, which allows different gases to diffuse through at different rates when different partial pressures are applied on either side. Gas absorption membranes have a simpler film with an absorption agent on one side and the flue gas on the other. Membranes for carbon dioxide separation are usually formed as hollow fibers arranged in the tube-and-shell configuration, or as flat sheets, which are typically packaged as spiral-wound modules.Compared to absorption separation, the advantages of the membrane process are [18, 19]:

- It does not require a separating agent, thus no regeneration is required;
- The systems are compact and lightweight, and can be positioned either horizontally or vertically, which is especially suitable for retrofitting applications;
- Modular design allows optimization of process arrangement by using multi-stage operation; and
- Low maintenance requirements because there are no moving parts in the membrane unit.

The commercial membranes for $CO_2$ separation are mainly prepared from cellulose

acetate, polysulfone, and polyimide. These membranes are primarily tailor-made for natural gas processing and not specifically developed for flue gas separation. The selectivity of $CO_2/N_2$ of these membranes is generally in the range of $20 \sim 40$, depending on the operating temperature. However, a new aminosilicate, sol-gel derived microporous inorganic membrane developed for enhanced $CO_2$ separation applications shows the highest $CO_2/N_2$ separation factor was in the range 100-200.[25]The membrane technology for flue gas application can be competitive with respect to chemical absorption if $CO_2$ flue gas concentration is higher than 10% [25].

**Hybrid Membrane and Amine Processes:**

It is desired to apply amine and membrane technologies in tandem, thereby forming a hybrid process, to capture $CO_2$ from flue gas. Micro-porous hollow fiber membranes are evolving as a new technology for $CO_2$ separation using amine-based chemical absorption processes. Micro-porous membranes are used in the gas-liquid unit where the amine solution is contacted with the $CO_2$ containing flue gas [25]. The principle advantage of the micro-porous membrane is the reduction in the physical size and weight of the gas-liquid contacting unit. Unlike conventional membrane separation, the micro-porous hollow fiber membrane separation is based on reversible chemical reaction, and mass transfer occurs by diffusion of the gas through the gas/liquid interface just as in the traditional contacting columns.

The hollow fiber membrane itself does not contribute to the separation but instead acts as a contacting medium between the gases the liquid. There are a number of advantages to using the gas-liquid membrane contactors, including [19]:

- High gas/liquid contact area due to the high packing density of the hollow fibers (500 to 1,500 $m^2/m^3$ versus 100 250 $m^2/m^3$ for a conventional column).
- Foaming is eliminated because the gas flow does not impact the solvent and there is no connective dispersion of gas in the liquid.
- The membrane acts as a partition between the gas and liquid, and the gas/liquid flow rate ratio may vary in a wide range without causing flooding problems.

- The process can tolerate a wider range of process condition variations, as the available gas/liquid contact area is not disturbed by variations in flow rates.
- Solvent degradation is minimized as oxygen (a degradation agent to amines) is prevented from intimate contact with the solvents.

**Mineralisation:**

The process involves the trapping of $CO_2$ streams in minerals containing Magnesium (Mg) or Calcium (Ca) to form carbonates. There are a range of appropriate minerals, but the most promising are ultramafic rocks, of which the most common are called serpentine and olivine. These are found in large quantities all over the world. The active component for this process is magnesium oxide (MgO), which constitutes some 30% of these rocks by weight. There are a number of advantages to this approach to $CO_2$ removal:

- These carbonates are a lower energy state than $CO_2$, which means that their formation is inherently permanent and stable.
- Ultramafic rocks are ubiquitous, so their use is possible just about everywhere.
- The process of trapping the $CO_2$ is exothermic i.e. it gives out heat so to some extent the process fuels itself.
- The materials produced are inert and can be used in making bricks and concrete, and as a component in production of a range of products including paint, paper, some plastics and ceramics.

However, a major disadvantage of this process is the quantity of material needed. Roughly 2 tonnes of serpentine are required to capture 1 tonne of $CO_2$. This means that capturing the $CO_2$ output of the power plant sector would require the mining, processing and disposal of 2 billion tonnes of ultramafic rock per year. The other major problem is of handling of such a large material streams.

**Distillation:**

Low temperature distillation (cryogenic separation) is a commercial process commonly used to liquefy and purify $CO_2$ from relatively high purity >90% sources. It involves cooling the gases to a very low temperature so that the $CO_2$ can be liquefied and separated. A gas stream can be similarly distilled to extract $CO_2$. However, since the boiling point of liquid $CO_2$ is -79°C (and that other gas in air is still lower) cooling the flue gas is extremely energy intensive. It does offer a good separation of $CO_2$ from flue gases containing fairly high concentrations typically 50-70%İt is also more effective for separation of $CO_2$ under high pressure. Since it produces liquid $CO_2$ this needs no further compression for transportation.[18, 19]

**Fixation by algae:**

Carbon dioxide can be removed from gas streams by Algae through photosynthesis. $CO_2$ rich gas streams are bubbled through tanks of micro-algae optimized for high $CO_2$ feeding. Algal culture for the $CO_2$ fixation requires a large amount of nutrients such as nitrogen and phosphorus compounds. Wastewater discharged from an industry can be used for algal cultivation. The main advantages of this process are [26, 27]:

- High purity $CO_2$ gas is not required for algae culture. It is possible that flue gas containing 2-5% $CO_2$ can be fed directly to the photobioreactor.
- Some combustion products such as $NO_x$ or $SO_x$ can be effectively used as nutrients for microalgae. This could simplify flue gas scrubbing for the combustion system.
- Microalgae culturing yields high value commercial products that could offset the capital and the operation costs of the process. Products of the proposed process are:
  (a) mineralized carbon for stable sequestration; and
  (b) compounds of high commercial value. By selecting appropriate algae species, either one or both can be produced.

- The proposed process is a renewable cycle with minimal negative impacts on environment. In practice the specific conditions required by the algae (not common at power stations) and the slow rate of carbon fixing mean this is not a realistic proposal at present.

Recently, a new technique which is combination of biological process and membrane separation process has been developed for removal of carbon dioxide.[26]

$CO_2$ **hydrates:**

Hydrates are structures in which gases are trapped in a crystalline solid similar in appearance to ice. They exist naturally (especially methane hydrates) in deep ocean formations. One suggested approach to trapping $CO_2$ is to dissolve flue gases in water under conditions that favors the formation of $CO_2$ hydrates. This typically occurs at temperatures around 0°C and pressures from 1 to 7 MPa. The $CO_2$ can then be released by lowering the pressure. This technique could prove useful in removing $CO_2$ from pressurised gas streams (e.g. from Integrated Combined Cycle Gasification) with very low energy loss. [19]

## 2.3 Adsorption phenomena:

### 2.3.1 Introduction:

Adsorption is a separation process in which certain components of fluid phase are transferred to the surface of the solid adsorbent. The phenomenon of adsorption was discovered over two centuries ago. The uptake of gases by charcoal was studied by C. W. Scheele in 1773 and by the F. Fontana in 1777. The adsorbing phase is the adsorbent, and the material concentrated or adsorbed at the surface of that phase is the adsorbate. Unlike Absorption in which solute molecules diffuse from the bulk of a gas phase to the bulk of a liquid phase, in Adsorption, molecules diffuse from the bulk of the fluid to the surface of the solid adsorbent, forming a distinct adsorbed phase. [28]

### 2.3.2 Mechanism of adsorption:

When the adsorbent is a porous media the transport of adsorbate to adsorbent will occur through three consecutive steps as mentioned in Figure 2.5 [29].

- Transport of solute from the bulk of the solution to the outer surface of the film surrounding the particle-bulk transport.
- Transport of solute within the film- film transport.
- Transport in the interior of the particle intra particle transport

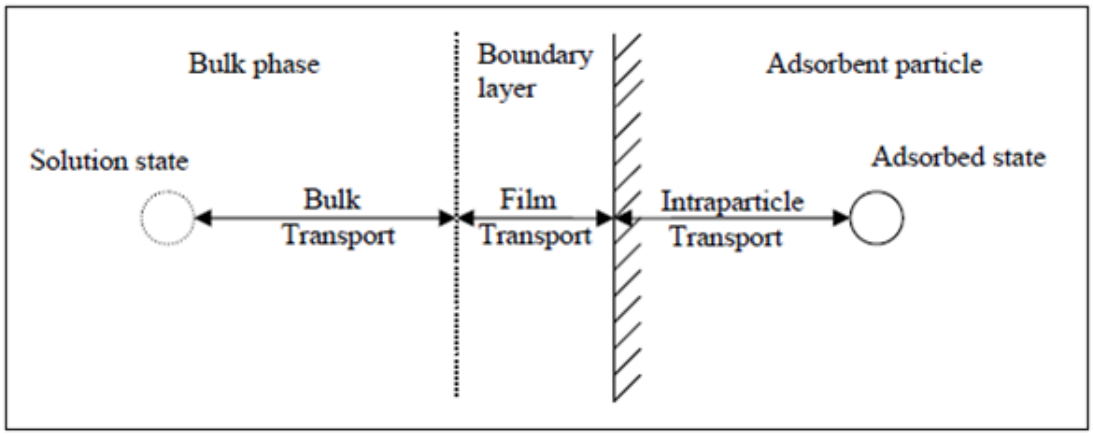


Figure 2.5: The transport of adsorbate to adsorbent

Two important properties in an adsorption system include the adsorptive capacity of a given amount of adsorbent for a particular solute and the adsorption rate at which that solute is taken out of solution. Adsorption rate depends on several factors mainly the size and porous structure of adsorbent particles, size and structure of the solute molecule, concentration of solute in solution, and temperature of solution. The surface chemical properties also play an important role for adsorbent. Factors including the gross surface area of the adsorbent, pore size, solubility of solute in aqueous solution, pH and temperature will affect the adsorptive capacity of the adsorbents.[29]

### 2.3.3 Types of Adsorption:

Adsorption can be distinguished into two types of phenomena: [27]

1. Physical adsorption

2. Chemical adsorption

**Physical adsorption (Physisorotion):**
Physical Adsorption is the result of intermolecular forces of attraction between molecules of the solid and the substance adsorbed. It is accompanied by low heat of adsorption with no structural changes occurring to the surface during the adsorption. In physisorption, multilayer adsorption takes place with increase in fluid concentration. The adsorbed substance does not penetrate within the crystal lattice of the solid and does not dissolve in it, but remains entirely upon the surface. It is an easily reversible phenomenon as the forces are not very strong and adsorbate can be removed from the surface by increasing the temperature and/or reducing the equilibrium pressure/concentration.

**Chemical Adsorption (Chemisorption):**
Chemical Adsorption is a result of the chemical interaction between the solid and the adsorbed substance. The strength of the chemical bond may vary considerably, and identifiable chemical compounds in the usual sense may not actually form, but the adhesive force is generally much greater than that found in physical adsorption. The heat liberated is usually large, of the order of the heat of chemical reaction. The process is frequently irreversible, and on desorption the original substance will often be found to have undergone a chemical change. The same substance which, under conditions of low temperature will undergo substantially only physical adsorption upon a solid will sometimes exhibit chemisorption at somewhat higher temperatures and both phenomena may occur at the same time [28, 29] .

### 2.3.4 Adsorption processes:

Large scale adsorptive separation processes may be divided into two broad classes; cyclic batch systems, in which the adsorbent bed is alternately saturated and regenerated in a cyclic manner, and continuous flow system, generally involving continuous countercurrent contact between feed and adsorbent. Cyclic batch processes differ from each other mainly in the methods by which the adsorbent is regenerated during the desorption cycle. Four basic methods which are in common use are described as follows [28] :

**Thermal swing:** In thermal swing operations the bed is regenerated by heating, usually with a stream of hot gas or liquid, to a temperature at which the adsorbed species are desorbed and removed from the bed in the fluid stream.

**Pressure swing:** In a pressure swing process desorption is accomplished by reducing the pressure at essentially the bed at low pressure. This mode of operation is obviously restricted to gaseous systems.

**Purge gas stripping:** In this method of regeneration, bed is regenerated at essentially constant pressure and temperature by purging with a non adsorbing inert gas. It is applicable only when the adsorbed species are weakly held, otherwise the quantity of purge required would be prohibitive. The desorbate is normally present only at very low concentrations in the purge gas so the method can not be used where the desorbate is to be recovered.

**Displacement desorption:** The temperature and pressure are maintained essentially constant, as in purge gas stripping, but instead of inert purge the adsorbed species are displaced by a stream containing a competitively adsorbed species. The method is applicable to both gas and liquid systems.

### 2.3.5 Basic type of industrial adsorbents:

Several commercially industrial adsorbents, their characteristics and applications are given in Table 2.3 . The major types of adsorbents used are activated alumina, silica gel, activated carbons, zeolites and polymeric adsorbents. In selecting the appropriate adsorbent for a specific application the following criteria should be met: The adsorbent should demonstrate high selectivity to the gas species to be separated ($CO_2$ in this case), high capacity to minimize the amount of adsorbent needed, fast adsorption kinetics, chemical and thermal stability, capacity of being easily regenerable and being of relatively low cost.[30]

Table 2.3: Commercially important adsorbent and their characteristics

| Adsorbent | Characteristics | Commercial use | Strengths | Weakness |
|---|---|---|---|---|
| Activated carbon | Hydrophobic surface,favours organic over air or water | Removal of organic pollutants from aqueous or gaseous effluents | Cheapest hydrophobic adsorbent,workhorse of pollution control | Difficult to regenerate if fouling occurs, may catch fire during air regenaration |
| Carbon molecular sieve (CMS) | Separates on the basis of difference in intraparticle diffusivity | Production of $N_2$ from air | The only practical adsorbent for selective adsorption of $O_2$ over $N_2$ | The only commercial application is in air separation |
| Silica gel | High capacity, hydrophilic adsorbent | Drying of air and other gases | Higher capacity than zeolite molecular sieves (ZMS) | Not very effective if the moisture level has to be reduced to very low |
| Activated alumina | High capacity, hydrophilic adsorbent | Drying of gas streams | Higher capacity than ZMS | Not as effective as ZMS for the removal of moisture in traces |
| Zeolite molecular sieve (ZMS) | Hydrophilic surface, polar regular channels | Dehydration, air separation, separation of molecules based on size and shape | Separation of molecules based on both polarity and geometry | Lower adsorption capacity than many other adsorbents |
| Silicalite | Hydrophobic surface | Removal or organics form gas streams | Can be regenerated by burning more easily | Quite expensive |

The commercial adsorption processes for separating gas and liquid mixtures are accomplished due to selective adsorption of certain substances from their mixtures. The same idea is true for purification of gas and liquid mixtures and drying of some industrial gases. For those purposes, the pore system of adsorbents used is sufficiently wide to enable fast diffusion; separation is caused mainly by selective adsorption that depends upon the van der Waals forces between the adsorbent and the constituents of the gas or liquid mixtures. Adsorptive separation and purification are also realized

in terms of both steric and kinetic mechanisms. Both of them are usually treated as equilibrium separation processes.[32]

Research has demonstrated that only activated carbon and zeolites can find applications in $CO_2$ separation. In general, molecular sieves have the higher capacity to adsorb $CO_2$ in terms of per unit weight compared with active carbons. Most physical $CO_2$ adsorbents such as 13X zeolite,[33] activated carbons,[34] unmodified periodic mesoporous silicas,[35]and metal-organic frameworks (MOFs)[36] require large pressure and/ or temperature gradient between the adsorption and desorption stages to enable both efficient adsorption performances and near complete desorption of $CO_2$. Moreover, they exhibit relatively low selectivity toward $CO_2$ and generally low tolerance to water vapor in the gas feed, and their $CO_2$ separation performance decreases drastically at increasing temperature. Essentially, adsorption of $CO_2$ using basic adsorbents requires high pressure operation, hence modified adsorption routes need to be developed with higher adsorption capacity, less energy and cost intensive. This can be achieved by two ways, namely (i) modification of adsorbents and (ii) development of nano-structured adsorbents.

### 2.3.6 Modification of adsorbents:

Most of the conventional adsorbents have low selectivity and capacity for $CO_2$ adsorption. Moreover, they require high energy in adsorption-desorption cycle. Therefore, there is a need to improve capacity and selectivity of these adsorbents. Some efforts have been made in this direction as summarized in Table 2.4 . A promising approach for $CO_2$ adsorbents that has been developed in recent years is the incorporation of amines into a high surface area support[37, 38, 39], combining good capacity and selectivity at moderate temperature. The presence of the surface-bound amine groups is thought to provide such materials with a selective affinity for $CO_2$ via the formation of ammonium carbamate species under anhydrous conditions and, in addition, via transformation to ammonium bicarbonate and carbonate species in the presence

of water.

Table 2.4: Modification of adsorbents

| Adsorbents type | Modifier | Characteristic of adsorbents | Reference |
|---|---|---|---|
| Zeolites (Zeolite 13X, $\beta$-Zeolite) | Monoethanol amine (MEA), Ethylene Diamine (ED), Isopropanolamine (IPA) | BET surface area and total pore volume decrease with amine loading, High $CO_2$ adsorption capacity at higher temperature as compared to bare zeolite, High selectivity for $CO_2$ over $N_2$ | [40, 41, 42] |
| Activated Carbon | Diethylenetriamine (DETA),Pentaethylenehexamine (PEHA),Polyethyleneamine (PEI),Aqueous suspension of metal oxides like $Cr_2$O and $Fe_2O_3$ | Drastic decrease in BET surface area, $CO_2$ adsorption capacity was reduced at room temperature, 80% regeneration after various adsorption-desorption cycles at room temperature | [43, 44] |
| Silica (Monolithic Silica) | Polyethylenimine (PEI), Tetraethylenepentaamine (TEPA) | BET surface area and total pore volume decrease with amine loading,High $CO_2$ adsorption capacity at higher temperature (75 °C),Retained adsorption capacity over various adsorption-desorption cycles | [45] |

Zeolite 13X had been modified with monoethanol amine (MEA) using methanol as the solvent. The adsorbent had been characterized for crystallinity, surface area, pore volume, and pore size. The $CO_2$ adsorption capacity of adsorbents was evaluated using the breakthrough adsorption method in the temperature range of 30-120 °C. The adsorbents showed improvement in $CO_2$ adsorption capacity over the unmodified ze-

olite by a factor of 1.6 at 30°C, whereas at 120°C the efficiency improved by a factor of 3.5. The adsorbent was also studied for $CO_2$ selectivity over $N_2$ at 75°C. The MEA modified adsorbent had selectivity for $CO_2$ over $N_2$ 1.4 times more compared to bare zeolite 13X. The performance of the adsorbent was also satisfactory in repeated cycles of adsorption.[40]

Li et al. (2008) developed a novel adsorbent by coating polyethylenimine (PEI) on glass fiber matrix and using epichlorohydrin as cross-linking agent. The physicochemical properties of the fibrous adsorbent were characterized. The experimental results showed that this fibrous PEI adsorbent exhibited much higher adsorption capacity of 3.98 mmol $CO_2$/g at 30°C. Factors that affect the adsorption capacity of the fibrous adsorbent were studied. The adsorbent can be completely regenerated at 120°C. This PEI-modified fibrous adsorbent had high thermal stability (about 250°C) and is stable in the presence of moisture[46].

Study by Chatti et al.(2009) describes the feasibility of amine loaded zeolites for $CO_2$capture. Novel functionalized adsorbents had been synthesized by immobilization of various amines like monoethanol amine, ethylene diamine and isopropanol amine on synthetic zeolite 13X. Effect of various parameters like effect of solvent, shaking time, synthesis temperature, and wetting of pellets prior to amine loadings was also studied. The adsorption capacities obtained were 0.36 mmol/g of $CO_2$ at 75°C for unmodified $\beta$-zeolite 13X and 0.45, and 0.52 mmol/g of $CO_2$ at 75°C for zeolite modified with monoethanol amine, and isopropanol amine[41].

Xu et al.(2009) synthesized a new type of composite adsorbents by incorporating monoethanol amine into $\beta$-zeolite. The adsorption behavior of carbon dioxide ($CO_2$), methane ($CH_4$), and nitrogen ($N_2$) on these adsorbents was investigated at 30°C. The results showed that the structure of zeolite did not deteoriate after MEA modification. In comparison with $CH_4$ and $N_2$, $CO_2$ was preferentially adsorbed on the adsorbents investigated. The introduction of MEA significantly improved the selectivity of both $CO_2/CH_4$ and $CO_2/N_2$. Very high selectivity of $CO_2/N_2$ of 25.67 was obtained on 40 wt% of MEA-functionalized beta-zeolite (MEA(40)-beta) at 1 atm and 30°C. Steric

effect and chemical adsorbate-adsorbent interaction were responsible for such high adsorption selectivity of $CO_2$. The adsorption capacity was constant after 6 cycles of adsorption and desorption [42].

Chen et al. (2009) prepared monolith silica with a hierarchical pore structure. It was impregnated with polyethylenimine (PEI) and tetraethylenepentaamine (TEPA). Amine-impregnated monolith silica exhibited significantly higher $CO_2$ adsorption capacity than other silica-supported amine sorbents, and produced a reversible and durable sorption performance. In particular, the PEI/monolith exhibited very reversible and durable $CO_2$ capturing performance (4.77 mmol/g of $CO_2$ at 75°C), and also showed excellent performances in both diluted and moisture-containing $CO_2$ conditions[45].

In the work done by Plaza et al.(2007) different alkylamines were evaluated as a potential source of basic sites for CO2 capture, and a commercial activated carbon was used as a preliminary support in order to study the effect of the impregnation. Diethylentriamine (DETA), pentaethylenehexamine (PEHA), and polyethylenimine (PEI) were used for impregnation. The amine coating increased the basicity and nitrogen content of the carbon. However, it drastically reduced the microporous volume of the activated carbon, which was chiefly responsible for $CO_2$ physisorption, thus decreasing the capacity of raw carbon at room temperature. Vacuum swing adsorption was applied to the prepared impregnated carbons. They do not achieve complete regeneration because of the chemisorptions character of these adsorbents.[43]

Li et al. (2008) prepared a novel fibrous adsorbent for $CO_2$ capture by coating polyethylenimine (PEI) on a glass fiber matrix, using epoxy resin (EP) as crosslinking agent. Factors that affected the adsorption capacity of the fibrous adsorbent were studied, including the crosslinking agent dosage, coating weight, moisture, adsorption temperature, and $CO_2$ concentration of the simulated flue gas. The experimental results indicate that the properly crosslinked fibrous adsorbent had a high thermal stability at about 280°C. Adsorption capacity of 2.02 mmol/g $CO_2$ was obtained at 30°C. Moisture had a promoting influence on the adsorption of $CO_2$ from flue gas.

The $CO_2$ adsorption capacity of the fibrous adsorbent in the presence of moisture could be 19 times higher than that in dry conditions. The fibrous adsorbent could be completely regenerated at 120°C.[54]

Chang et al. (2009) examined the characteristics and $CO_2$ adsorption capacity of mesoporous silicas including MCM-41, SBA-15, and pore expanded MCM-41 with pore size in a range of 2-17 nm. These mesoporous silicas were modified by mono-, di-, and tri-aminosilanes. SBA-15 was found to be a better support than MCM-41 and pore expanded SBA-15 for grafting amine onto the mesoporous silicas. SBA-15, possessing a proper pore size, accommodated amines and exhibited the best $CO_2$ adsorption capacity as 2.41mmol/g of $CO_2$ at 60°C. Selectivity of $CO_2/N_2$ of 0.66 at 30°C was obtained for tri-amine grafted SBA-15. Prepared amine-grafted SBA-15 exhibited better $CO_2$ adsorption capacities compared with other amine-grafted mesoporous silicas and zeolite 13X. [44]

Low cost carbon materials derived from fly ash were studied by Arenillas et al. (2005) for $CO_2$ adsorption through impregnation with organic bases like polyethylenimine aided by polyethylene glycol, tetraethylene-pentaamineacrylonitrile (TEPAN) and diethanolamine (DEA). The results showed that for same substrate, impregnated with different amines, the $CO_2$ adsorption capacities were relatively high (from 0.91 to 1.36 mmol/g of $CO_2$) especially at high temperatures (75°C), where commercial active carbons relying on physi-sorption had low capacities. The addition of PEG into the PEI-loaded adsorbents not only increased the $CO_2$ adsorption capacity but also decreased the time taken for the sample to reach equilibrium, i.e. become saturated with $CO_2$. Adsorbent retained the capacity after an adsorption-desorption cycle.[48]

Impregnation of activated carbons by metal oxides can be an efficient way to improve the surface adsorption characteristics of activated carbons. The effect of impregnation of activated carbon with $Cr_2$O and $Fe_2O_3$ and promotion by Zn2+ on its adsorptive properties of $CO_2$ was studied by Somy et al.(2009)[44]. Slurry and solution impregnation methods were used to compare $CO_2$ capture capacity of the impregnated activated carbon promoted by Zinc. The results showed that the amount of $CO_2$ adsorbed

on the samples impregnated by $Cr_2O$ was increased about 20% at 20°C as compared to raw activated carbon. It was found that $Fe_2O_3$ was not an effective impregnating species for activated carbon modification. Also slurry impregnation method showed higher $CO_2$ adsorption capacity in comparison with solution impregnation method. Samples prepared by co-impregnation of two metal species showed more adsorption capacity than samples impregnated by just one metal species individually. Washing the samples with distilled water after impregnation caused an increase adsorption capacity attributed to removal of metal oxides covering the surface physically and increases in surface area. Also, decreasing impregnation temperature from 95 to 25°C in solution method showed a significant increase in $CO_2$ adsorption capacity .[44]

Adsorption of $CO_2$ on triamine-grafted pore-expanded mesoporous silica, TRI-PE-MCM-41, was investigated by Belmabkhout et al. (2010) and Serna-Guerrero et al. (2010) from very low pressure to 1 bar at four temperatures. TRI-PE-MCM-41 exhibited one of the highest equilibrium capacities compared to other typical $CO_2$ adsorbents such as zeolites, activated carbons, and metal-organic frameworks. Also, TRI-PE-MCM-41 exhibited very small uptakes of $N_2$, $CH_4$, $H_2$, and $O_2$ showing high selectivity of $CO_2$ over other species even at very low $CO_2$ concentrations. Unlike most physical adsorbents the $CO_2$ adsorption capacity of TRI-PE-MCM-41 was improved in the presence of moisture. Adsorption-desorption cyclic measurements using pure $CO_2$ and $CO_2$-$N_2$ mixture showed excellent stability of the adsorbent upto 120°C.[30, 49]

Study by Chang et al. (2003) provided a novel approach for the preparation of high efficiency solid $CO_2$ sorbents. Mesoporous Silica SBA-15 was grafted with -(aminopropyl)triethoxysilane (APTS). SBA-15, with a uniform pore size of 21 nm and surface area of 200-230 $m^2$/g, provided an OH- functional group for grafting of APTS. Amine-grafted SBA-15 adsorbed $CO_2$ as carbonates and bicarbonates with a total capacity of 0.4 mmol/g. Repeated $CO_2$ adsorption and sorbent regeneration studies showed that amine grafted on SBA-15 exhibited hydrothermal stability and allowed repeated use without loss of $CO_2$ capture capacity.[50]

Maroto-Valer et al., (2008) developed activated fly ash derived sorbents for $CO_2$ capture. Fly ash carbon samples were steam activated at 850°C, resulting in a significant increase of the surface area (1075 $m^2$/g). The activated samples were impregnated with different amine compounds like monoethanol amine (MEA), diethanol amine (DEA), methyldiethanol amine (MDEA), and the resultant samples were tested for $CO_2$ capture at different temperatures. The $CO_2$ adsorption of the parent and activated samples is typical of a physical adsorption process. The impregnation process results in a decrease of the surface areas, indicating a blocking of the porosity. The highest adsorption capacity at 30 and 70°C for the amine impregnated activated carbons was probably due to a combination of physical adsorption inherent from the parent sample and chemical adsorption of the loaded amine groups. The $CO_2$ adsorption capacities for the activated amine impregnated samples are higher than fly ash carbons without activation.

Adsorption of pure $CO_2$ on SBA-15 impregnated with branched polyethyleneimine (PEI) has been studied by Sanz et al. (2010). Pure $CO_2$ adsorption isotherms on modified SBA-15 materials were obtained at 45°C, showing high adsorption efficiency for $CO_2$ removal at 1 bar. Chemisorption of $CO_2$ on amino sites of the modified SBA-15 seemed to be the main adsorption mechanism. $CO_2$ adsorption strongly depends on the PEI content of the silica material and the adsorption temperature of adsorption process, being possible to obtain a maximum adsorption value close to 2.04 mmol/g of $CO_2$ at 75°C and 1 bar. Adsorption capacity was also tested after regeneration of the PEI-impregnated SBA-15 materials. Results show that these branched PEI-impregnated materials are very efficient even at low pressure and after several adsorption-regeneration cycles.[51]

### 2.3.7 Adsorption equilibria and adsorption isotherms:

The adsorption of a substance from one phase to the surface of the another in a specific system leads to a thermodynamically defined distribution of that substance

between the phases when the system reaches equilibrium that is, when no further net adsorption occurs. The adsorption isotherm is the equilibrium relationship between the concentration in the fluid phase and the concentration in the adsorbent particles at a given temperature.

Experimental isotherms are useful for describing adsorption capacity to facilitate evaluation of the feasibility of this process for a given application, for selection of the most appropriate adsorbent, and for preliminary determination of adsorbent dosage requirements. Moreover, the isotherm plays a crucial functional role in predictive modeling procedures for analysis and design of adsorption systems. An additional potential use of adsorption isotherms is for theoretical evaluation and interpretation of thermodynamic parameters, such as heats of adsorption.

Six general types of isotherms have been observed by BDDT (Brunauer, Deming, Deming and Teller). Type I isotherms are typical of microporous solids where only monolayer adsorption occurs. In these, micropore filling occurs significantly at relatively low partial pressure $<0.1\mathrm{P}/P_O$, the adsorption process being complete at approximately 0.5 $\mathrm{P}/P_O$. Type II isotherms describe physical adsorption of gases by nonporous solids. Monolayer coverage is succeeded by multilayer adsorption at higher $\mathrm{P}/P_O$ values. Type III isotherms are confined to a few systems in which the overall adsorbent-adsorbate interactions are weak in comparison with relatively strong adsorbate-adsorbate interactions. Type IV and type V isotherms are convex towards the relative pressure axis. These isotherms are characteristic of weak gas-solid interaction. Type IV isotherms describe a multilayer adsorption process where complete filling of the smallest capillaries has occurred. Type IV isotherms originate from both non-porous and mesoporous solids and type V isotherms from microporous or mesoporous solids. The type VI isotherm, in which the sharpness of the steps depends on the system and the temperature, represents stepwise multilayer adsorptions on a uniform nonporous surface. The step-height now represents the monolayer capacity for each adsorbed layer and, in the simplest case, remains nearly constant for two or three adsorbed layers. [52]

Several model equations have been developed to describe adsorption isotherm relationships. These are as classified into to broad categories: Flat surface isotherm equations and Pore filling isotherm equations. The Flat surface isotherm equations include Langmuir isotherms, BET isotherms, Freundlich isotherms, Toth isotherms and Sips isotherms. The Pore filling isotherm equations include Dubinin-Radushkevich isotherm equation and Dubinin-Astakhov isotherm equation [53].

# Chapter 3

# Experimental Setup

Experimental methods used for adsorbent preparation, modification, characterization and evaluation have been described in this chapter.

## 3.1 Materials:

### 3.1.1 Alumina and Clay as support:

A composite of alumina 68 wt % and clay 32 wt % (ALC) was chosen as a support for the study and it has good surface area of 127 $m^2$/g, desired pore volume and size distribution. Before undertaking the preparation, the above alumina clay composite (ALC) was conditioned by drying and calcinations at 350°C. The modification of the surface chemistry of ALC was carried out by impregnating with sodium carbonate (SC), ($Na_2CO_3$). Various loadings of $Na_2CO_3$ have been carried out using wet incipient impregnation technique, where in the solution quantity equivalent to pore volume and solubility of solute would govern the loading of active component, in this case it is $Na_2CO_3$.

The modification of the surface chemistry of proprietary inorganic supports with sodium carbonate ($Na_2CO_3$) has been applied to generate a range of adsorbents.

Sodium carbonate (average molecular mass 106) was used and adsorbents were prepared using a wet incipient impregnation technique.
The adsorbents were prepared by loading $Na_2CO_3$ in different concentration of 5,10,15,20 and25 on the support material of alumina and clay (ALC) having a surface area of 127 $m^2$/gm, having an average particle size of 84 $\mu$m and 68% alumina.
The steps followed during the preparation of adsorbent are as follows:

- First the water pore volume is calculated for it 5 gm of support material was taken and it is dissolved in water then the water is filtered out and the adsorbent is dried in room temperature for 2 hours when all the water is dried from the surface the support material is again weighed and the increase in the weight is measured from it water pore volume was calculated. It came out to be 0.45ml/gm.

- Then as it came out 45 % in case of clay and alumina (ALC). I took 45 ml De mineralized water (D.M) in a beaker and $Na_2CO_3$ was taken according to the amount of loading needed to be prepared. That is if 5% loading need to be prepared 5 gm of $Na_2CO_3$ is taken and a solution is prepared.

- Then needed amount of support material is taken for 5% loading 95gm of support material is taken.

- Then we mix the solution prepared earlier to the support at once and then mixing the paste thoroughly.

- After good mixing the sample prepared is kept into the oven for heating it overnight at 110°C.

All the samples having ALC as support were prepared using the same steps. Higher loading of active component is achieved through successive impregnation stages. Impregnated samples are dried at 110°C overnight and labeled the sample as given in Table 3.1 .

Table 3.1: Labeling details of prepared samples with ALC as support

| Sample name | Support | $Na_2CO_3$ loading in wt% |
|---|---|---|
| ALC-SC-0 | ALC | 0 |
| ALC-SC-1 | ALC | 5 |
| ALC-SC-2 | ALC | 10 |
| ALC-SC-3 | ALC | 15 |
| ALC-SC-4 | ALC | 20 |
| ALC-SC-5 | ALC | 25 |

### 3.1.2 Transition Alumina as support:

A Transition Alumina (GAL) was chosen as the other support for the study as it has good surface area of 321 $m^2$/g, desired pore volume and size distribution. Before undertaking the preparation, the above (GAL) was conditioned by drying and calcinations at 350°C. The modification of the surface chemistry of GAL was carried out by impregnating with sodium carbonate (SC), ($Na_2CO_3$). Various loadings of $Na_2CO_3$ have been carried out using wet incipient impregnation technique, where in the solution quantity equivalent to pore volume and solubility of solute would govern the loading of active component, in this case it is $Na_2CO_3$. Higher loading of active component is achieved through successive impregnation stages. Impregnated samples are dried at 110°C overnight and labeled the sample as given in Table 3.2 .

Table 3.2: Labeling details of prepared samples with Transition-Alumina as support

| Sample name | Support | $Na_2CO_3$loading in wt% |
|---|---|---|
| GAL-SC-0 | GAL | 0 |
| GAL-SC-1 | GAL | 5 |
| GAL-SC-2 | GAL | 10 |
| GAL-SC-3 | GAL | 15 |
| GAL-SC-4 | GAL | 20 |
| GAL-SC-5 | GAL | 25 |

The modification of the surface chemistry of proprietary inorganic supports with sodium carbonate ($Na_2CO_3$) has been applied to generate a range of adsorbents. Sodium carbonate (average molecular mass 106) was used and adsorbents were prepared using a wet incipient impregnation technique. The adsorbents were prepared

by loading $Na_2CO_3$ in different concentration of 5,10,15,20 and25 on the support material Transition-Alumina (GAL). The steps followed during the preparation of adsorbent are as follows:

- First the water pore volume is calculated for it 5 gm of support material was taken and it is dissolved in water then the water is filtered out and the adsorbent is dried in room temperature for 2 hours when all the water is dried from the surface the support material is again weighed and the increase in the weight is measured from it water pore volume was calculated. It came out to be 0.45ml/gm.

- Then as it came out 45 % in case of Transition-Alumina (GAL). I took 45 ml De mineralized water (D.M) in a beaker and $Na_2CO_3$ was taken according to the amount of loading needed to be prepared. That is if 5% loading need to be prepared 5 gm of $Na_2CO_3$ is taken and a solution is prepared.

- Then needed amount of support material is taken for 5% loading 95gm of support material is taken.

- Then we mix the solution prepared earlier to the support at once and then mixing the paste thoroughly.

- After good mixing the sample prepared is kept into the oven for heating it overnight at 110°C.

## 3.2 Surface area and pore size distribution:

The surface area, pore size distribution and pore volume of samples were measured using a static volumetric system (Micromeritics Instrument corporation, USA, model ASAP 2020) shown in Figure 3.1 . For the characterization Nitrogen adsorption isotherm at 77K (under liquid nitrogen) in the pressure ranging from 0.1 to 850 mmHg was measured. As the presence of water and other adsorbed gases significantly

affects the validity of the $N_2$ adsorption measurement, the samples were activated by increasing the temperature at a heating rate of 1°C/min to 423 K under vaccum of about 10 mmHg and samples were maintained at 423K for 2 hours.

Table 3.3: Instrument and their make

| Parameters | Instruments | Make |
|---|---|---|
| BET Surface Area | ASAP 2020 | Micromeritics |
| Pore Volume | ASAP 2020 | Micromeritics |
| Pore Size | Mastersizer2000 | Micromeritics |

The total pore volume was calculated from the amount of Nitrogen adsorbed at relative pressure of 0.97. The total surface area was calculated using multi point Brunauer-Emmett and Teller (BET) surface area method. The pore size distribution was calculated by the Barrett- Joyner- Halenda (BJH) method.

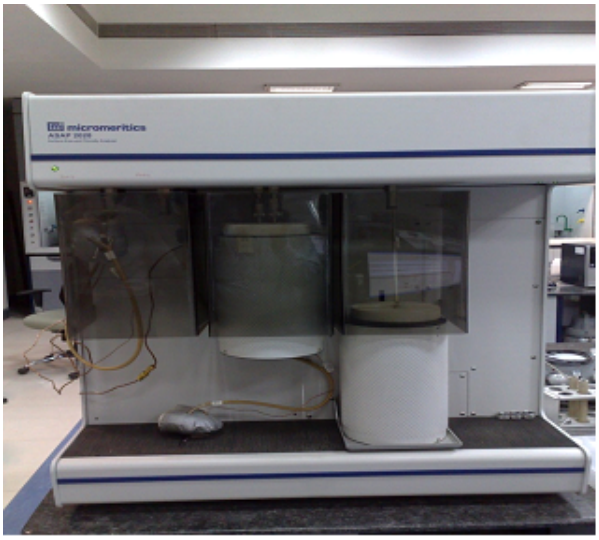


Figure 3.1: Surface area ASAP 2020

## 3.3 Experimental Setup used for $CO_2$ adsorption studies:

Experimental setup Figure 3.2 consists of a fixed bed down flow reactor with good temperature and flow control systems. Reactor material of construction is stainless steel. System consists of three gas lines with proper MFC and other control units to deliver desired flow of nitrogen or $CO_2$.To mix the gases uniformly back pressure and also turbulence was created by introducing gas filtration catridges in the flow lines. This reduced the variation and erratic reading of $CO_2$ detector. A bubbler (13) was fixed after filter catridge as shown in figure to introduce moisture along with reaction mixture, which would be one of the ingredients to set oxidation and reduction process to set. A carbon dioxide cylinder was set up with the help of a three way valve to pass the carbon dioxide into the setup. The gases coming out of the setup is sent to an online analyzer(20) as shown in Figure 3.2 . This gives the reading in volume percent of carbon dioxide coming out of the reactor.
Following procedure was followed for carrying out the experimental runs.

- A bed from glass wool is prepared and it is kept at the bottom of the reactor over which we put our adsorbent.
- After putting our adsorbent at place that is at the bottom of the reactor we start the flow of Nitrogen and also increase the temperature simultaneously to the set point.
- After the set temperature is attained then we start the flow of Carbon dioxide from the cylinder the flow of both Nitrogen and Carbon dioxide is controlled by the help of Mass flow controller (MFC).
- For making a uniform composition of nitrogen and carbon dioxide mixtures are provided so that the gases going into the reactor is properly mixed and having a uniform composition.

- The flow is maintained in such a way that the composition of carbon dioxide in the mixture gases going into the reactor remain at a desired value.
- After the flow is started then with the help of an online analyzer the concentration of carbon dioxide in the gases coming out from the reactor is continuously recorded.
- The concentration of carbon dioxide in the gases coming out is recorded at the interval of every 1 minute.
- The reading from analyzer comes out in volume percent of carbon dioxide in the gases coming out from the reactor.
- From the reading the calculations were done to calculate the carbon dioxide content in gases coming out of the reactor.

The Experimental set up is shown in Figure 3.2

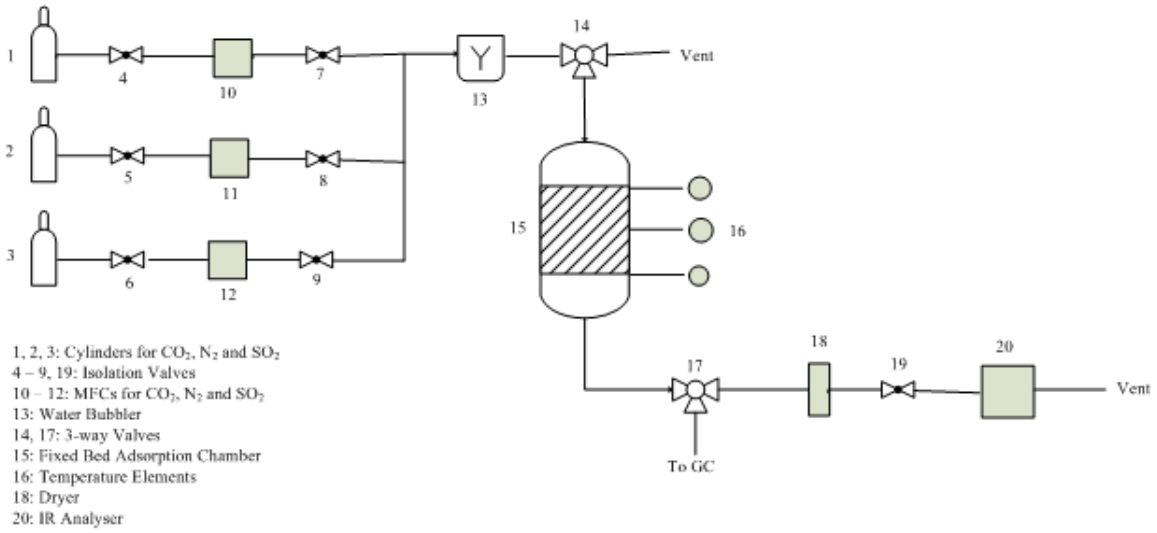


Figure 3.2: Experimental setup

## 3.4 Design of Experiment optimize the process parameters for $CO_2$ adsorption:

The design of experiment is based on factorial experimental design technique. In statistics, a full factorial experiment is an experiment whose design consists of two or more factors, each with discrete possible values or "levels", and whose experimental units take on all possible combinations of these levels across all such factors. A full factorial design may also be called a fully crossed design. Such an experiment allows studying the effect of each factor on the response variable, as well as the effects of interactions between factors on the response variable.

For the vast majority of factorial experiments, each factor has only two levels. For example, with two factors each taking two levels, a factorial experiment would have four treatment combinations in total, and is usually called a 2×2 factorial design.

If the number of combinations in a full factorial design is too high to be logistically feasible, a fractional factorial design may be done, in which some of the possible combinations (usually at least half) are omitted. To study the effect of process parameters and their surface interactions , we have considered 3 process variables at 3 levels and designed the experiments (DOE). Simulated flue gas with 3 - 9 vol% $CO_2$, 2.5 vol% $H_2O$ and balance $N_2$ is chemically adsorbed by the supported $Na_2CO_3$ at 55-70°C temperature to produce sodium bicarbonate ($NaHCO_3$) by the following reaction. $NaHCO_3$ is then regenerated at elevated temperature of 120 °C and above to produce concentrated $CO_2$ stream from the flue gas.

## 3.5 Reaction Chemistry:

**$CO_2$ Adsorption (Carbonation)**

$$Na_2CO_3\ (s) + CO_2(g) + H_2O(g) \rightleftharpoons 2NaHCO_3(s)$$

Exothermic $\Delta$Hr°= $-735$ kcal/kg $CO_2$ Operating temperature: <80°C

**Sorbent Regeneration**

$$2NaHCO_3(s) \rightleftharpoons Na_2CO_3(s) + CO_2(g) + H_2O(g)$$

Endothermic $\Delta$ Hr°= 735 kcal/kg $CO_2$ Operating temperature: >120 °C

The above reaction chemistry followed during the adsorption process. As we can see adsorption is carried out at comparatively lower temperatures and the basis of this adsorption and desorption process is the thermal swing adsorption. In thermal swing operations the bed is regenerated by heating, usually with a stream of hot gas or liquid, to a temperature at which the adsorbed species are desorbed and removed from the bed in the fluid stream. The contaminants also affect the operation of bed by the following reaction.

Contaminants

$$Na_2CO_3(s) + SO_2(g) + O_2(g) \rightarrow Na_2SO_4(s) + CO_2(g)$$
$$Na_2CO_3(s) + 2HCl(g) \rightarrow 2NaCl\ (s) + CO_2(g) + H_2O\ (g)$$

## 3.6 Isotherm:

Various isotherms for adsorption of gases on solids have been analyzed using different approaches such as Langmuir theory, BET theory, Polanyi's Potential theory. In addition, there are several semi-empirical approaches to describe the adsorption of gases on solids.

### 3.6.1 Langmuir isotherm:

However, the most commonly used model is Langmuir model that describes Type I isotherm and has been extensively used for adsorption of methane and $CO_2$ on coal. Langmuir model is based on the assumption that there exists a fixed adsorption sites on the surface of the solid and only one gas molecule is adsorbed at a single adsorption site. Moreover the adsorbent surface is energetically homogeneous and that the energy of adsorption is constant for all sites with no interaction between the adjacent adsorbate molecules. The equation for the Langmuir isotherm is given as:

$$\frac{1}{V} = (\frac{1}{KV_m} \times \frac{1}{P}) + \frac{1}{V_m} \tag{3.1}$$

V is the adsorbed volume at a given partial pressure P.$V_m$ is the Langmuir volume.K is Langmuir constant. As per the Langmuir model it is believed that the surface of the solid should be energetically homogeneous.

### 3.6.2 BET Isotherm:

In 1938, Brunauer et al., modified some of the assumption of Langmuir model and provided an extended Langmuir model for multilayer adsorption popularly known as the Brunauer, Emmet, and Teller (BET) model. This model assumes that the surface of the adsorbent is energetically homogeneous with no interaction between the

adsorbed molecules. Moreover, the heat of adsorption is equal to the molar heat of condensation in all layers except for the first layer which acts as a stack. At saturated vapor pressure, the adsorbate condenses to liquid on the surface of the solid leading to infinite layers. The BET isotherm equation is given as:

$$\frac{1}{V(P_0/P-1)} = \frac{1}{V_m \times C} + \frac{C-1}{V_m C} \times \frac{P}{P_0} \tag{3.2}$$

where, Vm is the monolayer volume, C is a constant, Po is the saturation vapor pressure, and the remaining variables have their usual meaning. Although BET equation does not entirely fit into the experimental data, yet it is a useful tool that provides a theoretical foundation for the various isotherms shapes. The validity for the BET model generally ranges between relative pressure values of 0.05 to 0.35.

### 3.6.3 Polanyi's potential theory of adsorption isotherms:

Polanyi's potential theory of adsorption assumes the existence of a potential field around the surface of the solid into which the adsorbed gas molecule falls. The adsorption potential is the work done per mole of adsorbate needed in transferring molecules from the gaseous state to adsorbed state. It implicates the work done by temperature-independent dispersion forces. Therefore the potential curve is independent of temperature, and is typical of the particular gas-solid system alone. It is a function of the enclosed volume surrounding the adsorbent surface. Hence, the adsorbed volume is a function of adsorption potential (A) alone given as:

$$V = f(A) \tag{3.3}$$

The above relation is typical of a gas-solid system, and is called the characteristic curve. The characteristic curve generated from one experimental isotherm thus helps to predict the isotherms at different temperatures. Considering the adsorbate behaves

as an ideal gas, the adsorption potential is given as:

$$A = RT \times ln\frac{P_0}{P} \tag{3.4}$$

where, R is the Universal Gas Constant, A is the adsorption potential, T is the adsorption temperature in absolute units, P is the adsorption pressure and Po is the saturated vapor pressure of the adsorbate at definite temperature T.

In 1967, Dubinin described adsorption on microporous adsorbents and proposed a new theory known as the theory of volume filling of micropore (TVFM).Thus the mechanism by which adsorption of microporous solid occurs is restricted to volume rather than their surface. Dubinin (1975) thus introduced a new theory called the Theory of Volume Filling of Micropore that postulates that, in micropores, the adsorbate occupies the pore volume by the mechanism of volume filling, and does not form discrete layers in the pores. Dubinin and Radushkevich proposed an equation based on this theory that represented the isotherms that obeyed the TVFM. The Dubinin-Radushkevich (D-R) equation, it is expressed as follows:

$$V = V_0 \times Exp[-Dln(\frac{P_0}{P})]^2 \tag{3.5}$$

where, V is the amount adsorbed, $V_o$ is the micropore volume, n is the structural heterogeneity parameter which is restricted to 2, D=(RT/$\beta$ E)n is a constant, where, E is the characteristic energy of the adsorption system, T is the absolute temperature, R is the Universal Gas Constant, and $\beta$ is the adsorbate affinity coefficient. D is a constant for a particular adsorbent-adsorbate system, and is determined experimentally. Po is the saturation vapor pressure of the adsorbate at temperature T, and P is the equilibrium free gas pressure.

# Chapter 4

# Results and discussion

This section of the thesis discusses the experimental results and the possible explanations with available scientific basis. To develop high capacity and re-generable adsorbent, Alumina clay and transition alumina were chosen as a carrier material, prepared $Na_2CO_3$ supported adsorbent, characterised and evaluated under different process conditions with simulated flue gas.

## 4.1 Sodium Carbonate deposited on ALC:

### 4.1.1 Surface area analysis:

The surface area and pore volume of all samples prepared was measured using a static volumetric system (Micromeritics Instrument Corporation, USA, model ASAP 2020). The surface area was calculated using multi point Brunauer- Emmett and Teller (BET) surface area method and the total pore volume was calculated from the amount of nitrogen adsorbed at relative pressure of 0.97.

The surface area and pore volume of the samples are given in the Table 4.1 below.

Table 4.1 data infers the decrease of surface area and pore volume with increasing $Na_2CO_3$ loading, indicating the deposition of solute on the surface area available from all the pores, which in turn clog the pores and decrease the pore volume and

Table 4.1: Surface area and Pore volume of the samples

| Sample name | Suface area ($m^2$/g) | Change in Surface Area ($m^2$/g) | Pore Volume ($cm^3$/g) | Change in Pore Volume ($cm^3$/g) |
|---|---|---|---|---|
| ALC-SC-0 | 127 | 0 | 0.345 | 0 |
| ALC-SC-1 | 112 | 15 | 0.321 | 0.024 |
| ALC-SC-2 | 96 | 31 | 0.310 | 0.035 |
| ALC-SC-3 | 85 | 42 | 0.309 | 0.036 |
| ALC-SC-4 | 81 | 46 | 0.271 | 0.074 |
| ALC-SC-5 | 71 | 56 | 0.255 | 0.090 |

surface area.

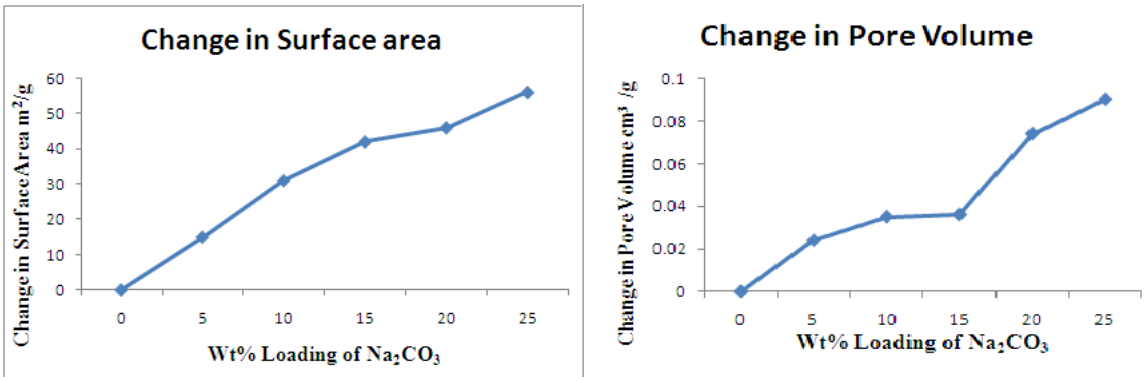


Figure 4.1: Change in Surface Area and Pore Volume

Decrease in surface area upto 20wt% loading of $Na_2CO_3$ with a particular rate and with higher loading of 25 wt% the rate of change in surface area increased drastically. Similar change can be seen from pore volume data also. Results indicate mono layer formation of $Na_2CO_3$ upto 15 to 20wt% and increased loading results in multilayer and agglomerated $Na_2CO_3$. As there is no contribution of surface area and pore volume coming from $Na_2CO_3$, one can assume that the $Na_2CO_3$ present on ALC was in fine crystalline form.

Figure4.2 gives the pore size distribution it shows a dual pore size distribution. ALC is the mixture of Alumina and Clay, smaller pores in the range 20- 100 Å are contributed

by alumina and the higher pores above 100Å are contributed by clay. ALC-SC series samples would be useful for the study of effect of pore size in regulating the diffusion of $CO_2$.

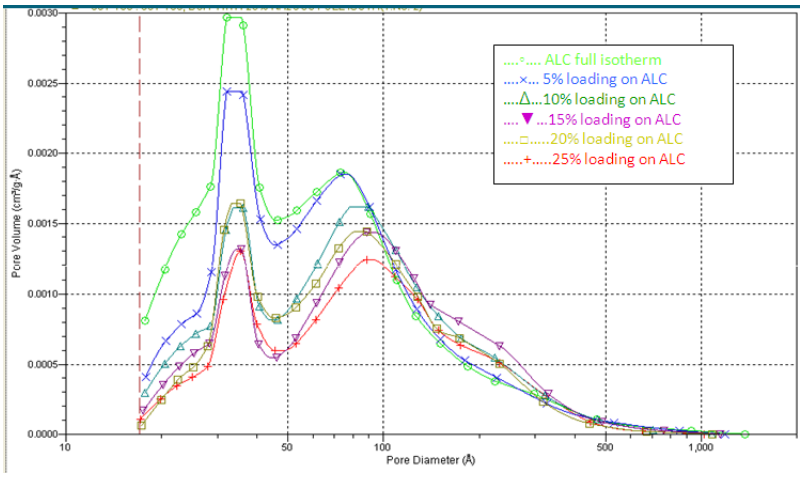


Figure 4.2: Pore size distribution of ALC

### 4.1.2 Effect of $Na_2CO_3$ Loading:

The breakthrough curves for virgin and alkali-impregnated sample ALC-SC-4 with different loading are are shown in Figure4.3 . There was an instrumental time lag of around 4 minutes after which $CO_2$ response was observed. $CO_2$ adsorption capacity has been used for screening and selecting the adsorbent for detail parametric study as per the DOE.

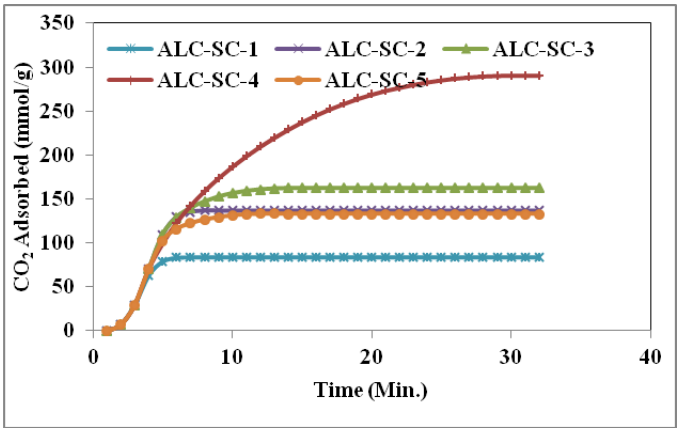


Figure 4.3: Comparison of $CO_2$ adsorption capacity of different adsorbents as a function of $Na_2CO_3$ loading at 8-vol% $CO_2$ concentration

The adsorption of $CO_2$ at close to atmospheric pressure requires adsorption through chemical redox processes there by sodium carbonate impregnated over inorganic supports to convert to $NaHCO_3$ sodium bicarbonate. Modification of support with sodium carbonate increases the affinity towards $CO_2$ capture from flue gases. Adsorption and desorption strength of $CO_2$ with active centre would determine the temperature requirement for adsorption and desorption. Difference in adsorption and desorption temperature is directly proportional to the energy requirement of the process. Our objective is to reduce the regeneration temperature, so that the process is more economical and energy efficient. Capacity of $CO_2$ adsorption per gram of adsorbent is mainly depend on the accessible carbonate concentration on the surface.

Means, the catalyst preparation method should be in such a way that the solute mono layer is ensured on the surface.Capacities for all adsorbents are depicted in Figure4.3 . Out of Alumina clay series ALC-SC-4 (20% $Na_2CO_3$ on ALC) is found to have the highest $CO_2$ adsorption capacity at 55°C Table 4.2 .

Table 4.2: Adsorption capacities of selected samples of alkali-impregnated ALC with 8 vol% $CO_2$ in simulated flue gas

| Sample ID | $Na_2CO_3$ loading in wt% | $CO_2$ Adsorbed in (mmol/g of Adsorbent)at 55°C | $CO_2$ Adsorbed in (mg/g of Adsorbent) at 55°C |
|---|---|---|---|
| ALC-SC-0 | 0 | 0.0 | 0.0 |
| ALC-SC-1 | 5 | 83.9 | 9.2 |
| ALC-SC-2 | 10 | 136.8 | 7.5 |
| ALC-SC-3 | 15 | 162.3 | 5.9 |
| ALC-SC-4 | 20 | 290.9 | 8.0 |
| ALC-SC-5 | 25 | 133.2 | 2.9 |

$CO_2$ uptake increases with increasing in carbonate loading up to 20 wt% and then drastically decreased at 25 wt% carbonate loading. If carbonate dispersion is one of the reasons for the above phenomena of decrease in $CO_2$ uptake, then the normalized values based on carbonate loading should decrease with increasing loading, which was presented in Table4.2 .The above trend of increasing $CO_2$ uptake with $Na_2CO_3$ loading was observed up to 15wt% to 20 wt% . To check the reproducibility of the above results, the experiments were performed three times under identical conditions. Results are reproducible with standard deviation of 5% as shown in Figure4.4 and Reproducibility of $CO_2$ adsorption experiments shows very good level of confidence i.e. 95% Table 4.3

Since the adsorption capacity for ALC-SC-4 (20% $Na_2CO_3$ on ALC) was highest and the results were reproducible to an accuracy level of around 95% the same adsorbent was selected for further detail parametric optimization study using DOE.

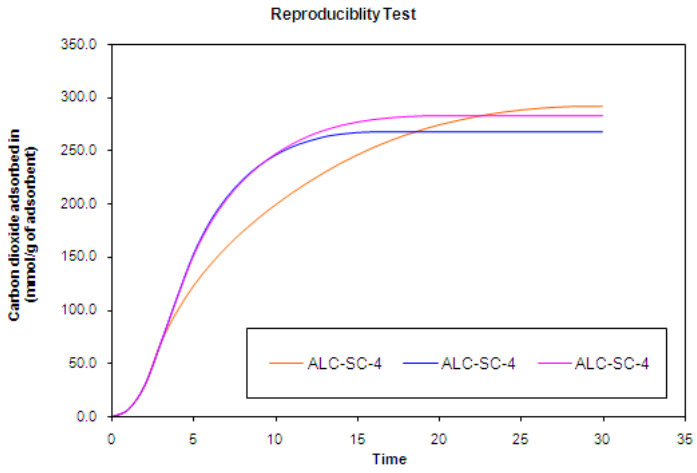


Figure 4.4: Reproducibility of ALC-SC-4 under similar condition

Table 4.3: Adsorption capacities of selected samples of alkali-impregnated ALC with 8 vol% $CO_2$ in simulated flue gas

| Temperature | Sample name | $Na_2CO_3$ loading | $CO_2$ Adsorbed in(mg/gm of adsorbent) | $CO_2$ Adsorbed in(mmol/gm of adsorbent) |
|---|---|---|---|---|
| 55°C | ALC-SC-4 | 20% | 13 | 291 |
| 55°C | ALC-SC-4 | 20% | 12 | 267 |
| 55°C | ALC-SC-4 | 20% | 12 | 283 |

### 4.1.3 Studies to optimize process parameters:

Statistical design of experimental methodology used to study the parametric optimization and surface response models development. DOE experimental plan was described in experimental section i.e, chapter 3.

Larger quantity of ALC-SC-4 sample was prepared in three lots and checked for the reproducibility of preparation and mixed to make common lot to carry out the study. In this study the effect of process parameters, we have considered were 3 process variables at 3 levels. Statistical design of experiments (DOE) was prepared by using Minitab software. Objective of the design of experiment is to provide correlations and interactions between various parameters. Simulated flue gas with 3, 6, 9 vol%

Table 4.4: Levels of DOE (Design of Experiment)

| Process parameter | Temperature | $CO_2$ concentration | Flow rate(ml/min) |
|---|---|---|---|
| Level 1 | 55 | 3 | 100 |
| Level 2 | 60 | 6 | 125 |
| Level 3 | 65 | 9 | 150 |

$CO_2$ with constant i.e, 2.5 vol% $H_2O$ and balance $N_2$. Flow rates varied during the study were 100, 125 and 150 ml/min. The mixture was chemically adsorbed by the supported $Na_2CO_3$ at 55 -70 °C temperature, which converts the carbonate to bicarbonate ($NaHCO_3$) of sodium. Adsorbent was then regenerated at elevated temperature of 120 °C and to produce concentrated $CO_2$ stream from the flue gas. Temperature required for the regeneration needs to finalize only after temperature programmed desorption study.

### 4.1.4 Effect of temperature :

Effect of temperature was studied at different flow rates with the same $CO_2$ concentration in simulated flue gases. Temperature was varied in a step of 5 °C starting from 55 °C.

Figure4.5 shows the results of $CO_2$ adsorption from flue gas containing 3% $CO_2$ .During the above experiment flue gas flow rate of 150ml/min was maintained. As per the experimental design temperature was varied in 5 °C steps. It has been observed that there was a negligible effect of temperature at low concentration of $CO_2$ in simulated flue gas stream. Reason for the above may be due to the lower partial pressure of $CO_2$ in the flue gas, making the population of active sites excess then the adsorbate i.e $CO_2$.

The similar observation was drawn in the case of 125 ml/min which was shown in the Figure 4.6 at different temperatures of 55, 60, and 65 °C. It has been observed that

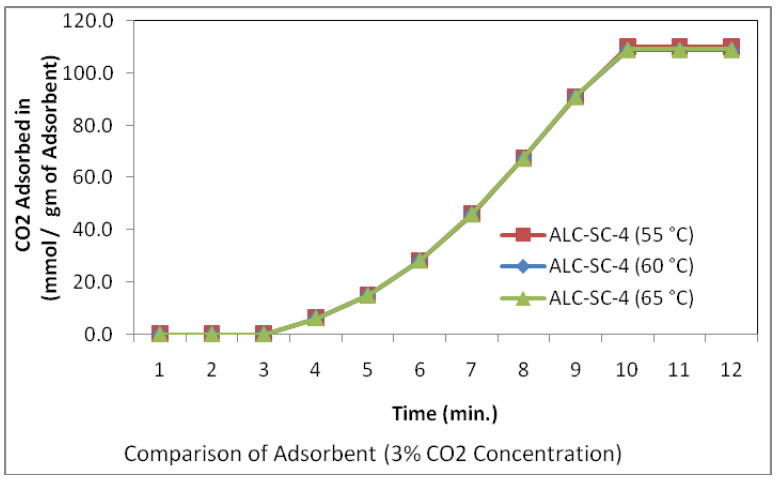


Figure 4.5: Comparision of adsorbent at 150 ml/min flow rate and 3% CO2 concentration

there was negligible effect of temperature with low concentration of $CO_2$ in simulated flue gas stream, which may be due to the lower partial pressure of $CO_2$ in the flue gas, making the population of active sites excess then the adsorbate.

The same trend was also seen when the flow was 100 ml/min the reason are the same as that were for the two previous simulated flows of 150 and 125 ml/min. The result is shown in Figure 4.7

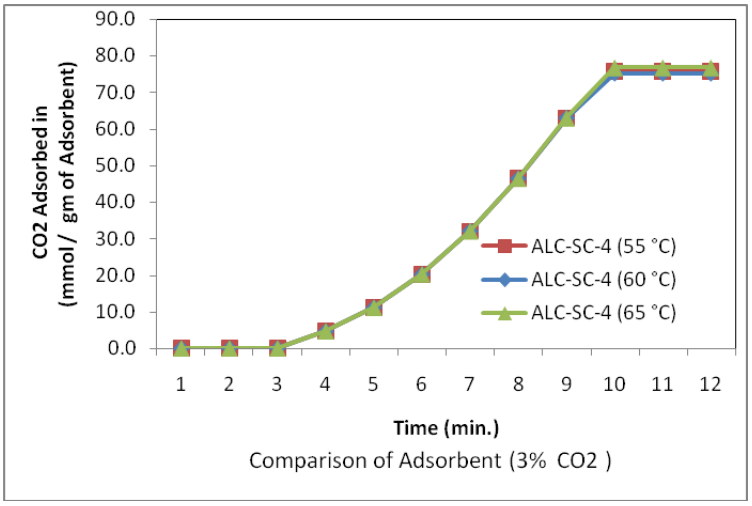


Figure 4.6: Comparision of adsorbent at 125 ml/min flow rate and 3% CO2 concentration

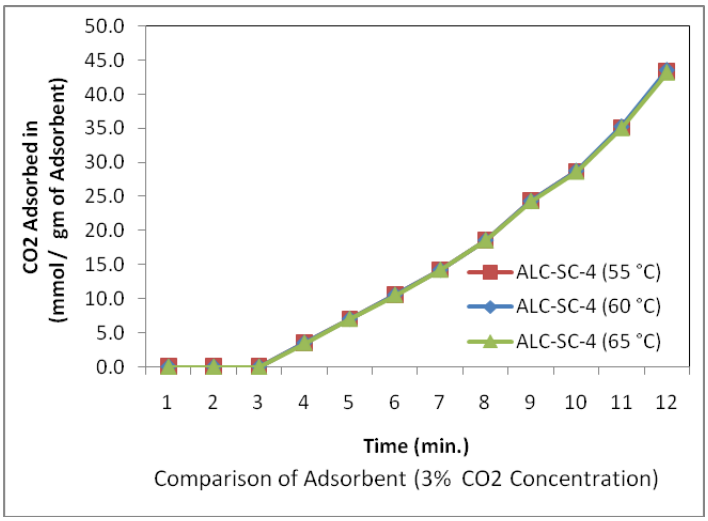


Figure 4.7: Comparision of adsorbent at 100 ml/min flow rate and 3% CO2 concentration

The above results infers that $CO_2$ concentration limits adsorption and may require different process conditions like lower temperatures and higher contact time. To find the optimized concentration of $CO_2$, the concentration was increased.

At 6% concentration of $CO_2$ in the simulated flue gas Figure 4.8 , which shows the variation in the adsorption of $CO_2$ at total flow rate of 150 ml/min at different temperatures 55, 60, and 65 °C. It has been observed that as the temperature increases the adsorption decreases from 55°C to 65°C which is in accordance with the literature. The adsorption decreases drastically when the temperature was increased by 5 °C. The adsorption rate was not changed much when the temperature was further raised to 65 °C, which may be due to setting up of desorption of $CO_2$.

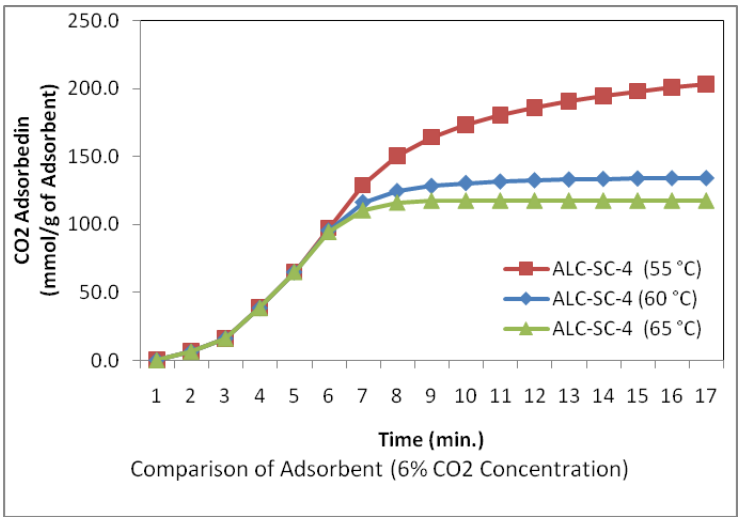


Figure 4.8: Comparision of adsorbent at 150 ml/min flow rate and 6% CO2 concentration

The Figure 4.9 depicts the adsorption of $CO_2$ at total flow rate of 125ml/min at different temperatures of 55, 60, and 65°C. The trend observed in case of 125 ml/min flow, the $CO_2$ adsorption decreases with increase in temperature. There was continuous drop in the adsorption of $CO_2$ for the increase in temperatures; this may be due to the high contact time between the $CO_2$ and adsorbent.

Slight difference in adsorption pattern was observed in the case of 100 ml/min flow

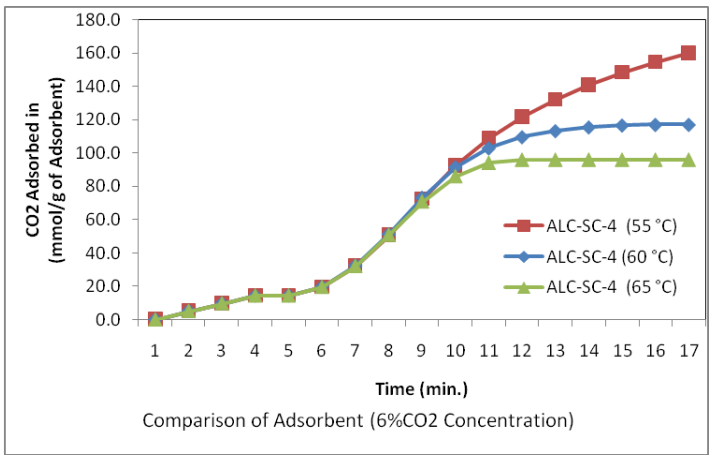


Figure 4.9: Comparision of adsorbent at 125 ml/min flow rate and 6% CO2 concentration

rate Figure 4.10 . The adsorption was increased in initial stage of experiment at 60 °C as a function of time (9 - 15 min) afterwards attaints the maximum adsorption as in the case of 55 °C. This may be due the inconsistency in bed packing.

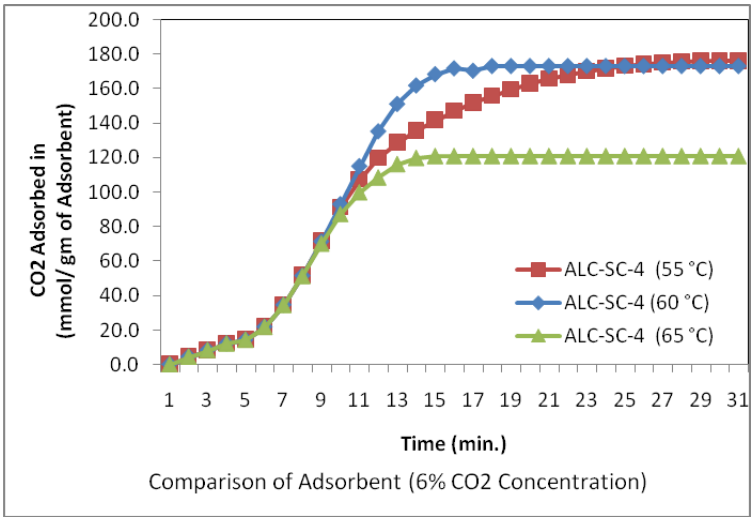


Figure 4.10: Comparision of adsorbent at 100 ml/min flow rate and 6% CO2 concentration

Further the concentration of $CO_2$ was increased to 9 % to find the maximum adsorption for $CO_2$ at different temperatures Figure4.11 . At 9 % $CO_2$ concentration the adsorption was 231 mmol/g as compared to the 6 % $CO_2$ concentration (216 mmol/g) at 55 °C, this is due to the increased partial pressure of $CO_2$. The similar trend was observed when the temperature was increased from 60 to 65 °C, which is because of the adsorption-desorption equilibrium.

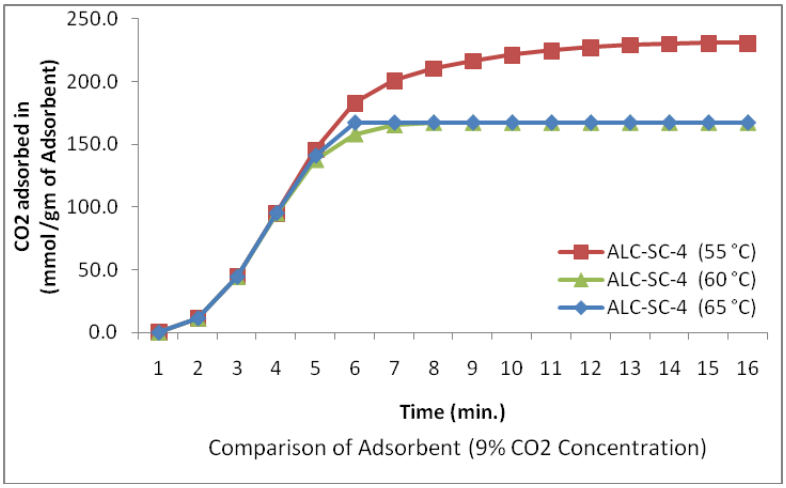


Figure 4.11: Comparision of adsorbent at 150 ml/min flow rate and 9% CO2 concentration

Figure 4.12 and 4.13 shows the adsorption pattern for CO2 at 125 and 100 ml/min flow rate respectively at 9 % concentration. The adsorption goes on decreasing as function of temperature.

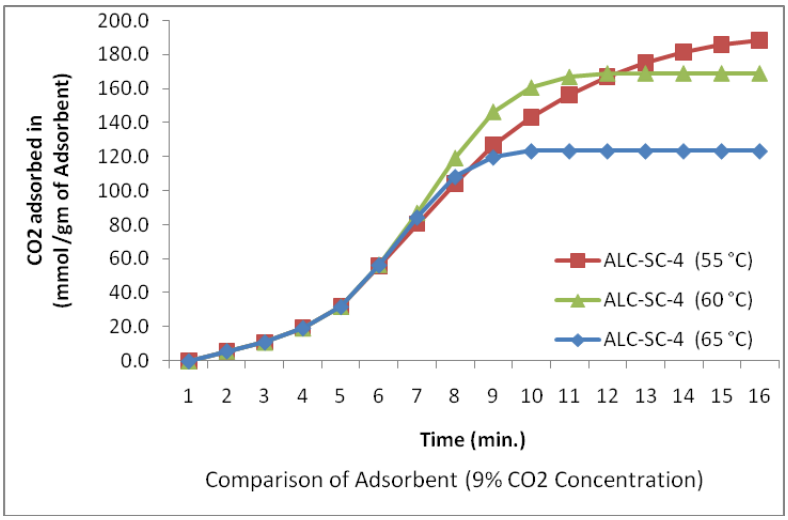


Figure 4.12: Comparision of adsorbent at 125 ml/min flow rate and 9% $CO_2$ concentration

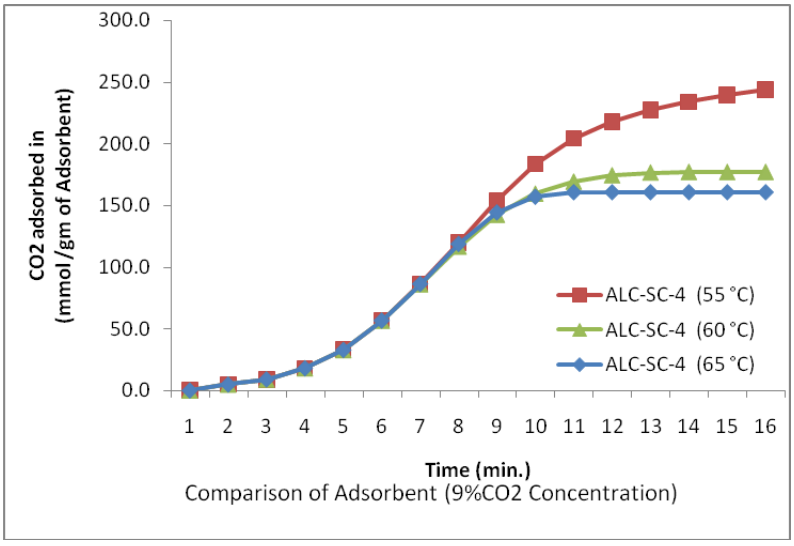


Figure 4.13: Comparision of adsorbent at 100 ml/min flow rate and 9% $CO_2$ concentration

The effects of different temperatures and $CO_2$ concentrations at a constant flow rate of 150 ml/min is given in Table 4.5 . It is very much clear for the values that the adsorption increases with increase in concentration and decreases with increase in temperature. This is due to the high contact time and desorption phenomenon at elevated concentration and temperature. It has been observed that there was a negligible effect of temperature with low concentration of $CO_2$ in simulated flue gas stream.

Same trend was seen when the flow rate was 125 ml/min and 100ml/min as shown

Table 4.5: Adsorption of CO2 at 150ml/min at different temperatures

| Carbon dioxide adsorbed in mmol/g of adsorbent | | | |
|---|---|---|---|
| Temperature°C | 9 volume % $CO_2$ | 6 volume % $CO_2$ | 3 volume % $CO_2$ |
| 55 | 231 | 216 | 110 |
| 60 | 168 | 134 | 109 |
| 65 | 161 | 117 | 109 |

in Table 4.6 and Table 4.7 respectively.

Table 4.6: Adsorption of $CO_2$ at 125ml/min at different temperatures

| Carbon dioxide adsorbed in mmol/g of adsorbent | | | |
|---|---|---|---|
| Temperature°C | 9 volume % $CO_2$ | 6 volume % $CO_2$ | 3 volume % $CO_2$ |
| 55 | 190 | 176 | 83 |
| 60 | 169 | 117 | 80 |
| 65 | 123 | 96 | 77 |

Table 4.7: Adsorption of $CO_2$ at 100ml/min at different temperatures

| Carbon dioxide adsorbed in mmol/g of adsorbent | | | |
|---|---|---|---|
| Temperature°C | 9 volume % $CO_2$ | 6 volume % $CO_2$ | 3 volume % $CO_2$ |
| 55 | 251 | 176 | 122 |
| 60 | 177 | 173 | 121 |
| 65 | 160 | 121 | 118 |

### 4.1.5 Model fitting for ALC-SC-4:

Various isotherms for adsorption of gases on solids have been analyzed at different temperatures under which the experiments were carried out that is at 55°C, 60°C, and 65°C using different approaches such as Langmuir theory, BET theory, Polanyi Potential theory.For the simplicity, the concentration of $CO_2$ been converted to partial pressure.The experimental data at 55°C was used to model the adsorption kinetics using Langmuir, D-R and BET models. The Langmuir, D-R and BET parameters were calculated and have been given below Table 4.8 . The comparison between experimental values and parametric Langmuir D-R and BET models for all the flow rates has been shown in Figure 4.14 to 4.16 .

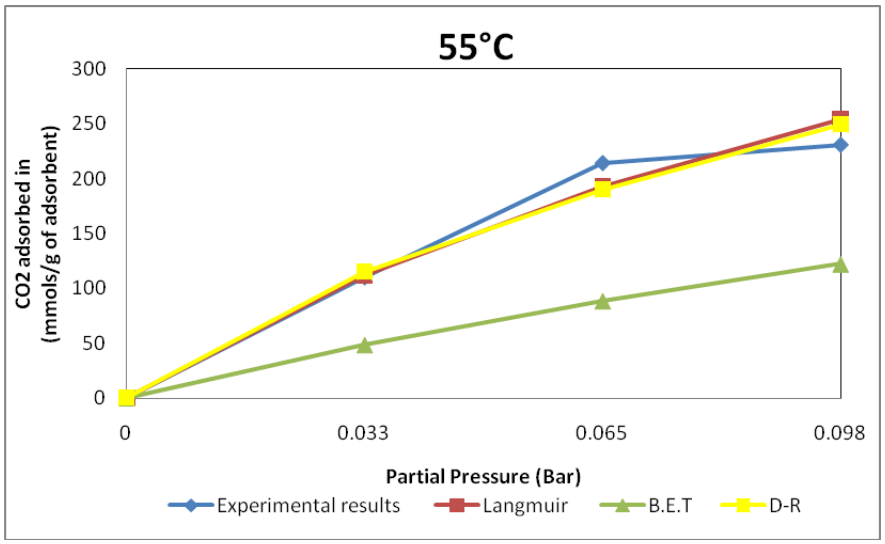


Figure 4.14: Comparison of experimental values with theoretical models for flow of 150ml/min at 55°C

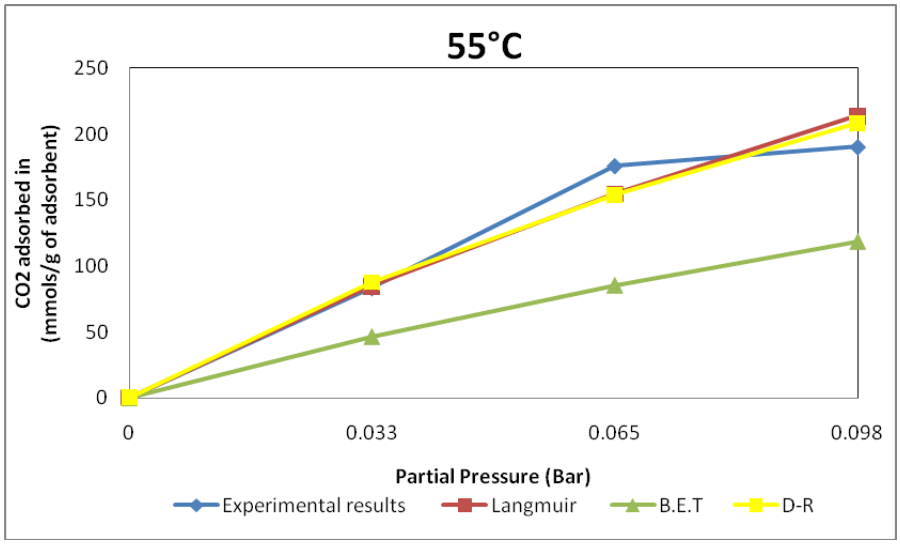


Figure 4.15: Comparison of experimental values with theoretical models for flow of 125ml/min at 55°C

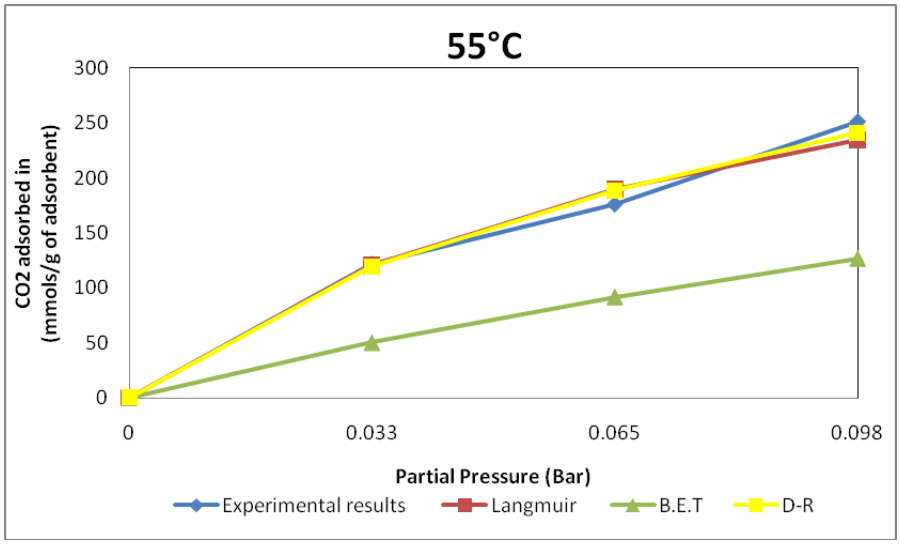


Figure 4.16: Comparison of experimental values with theoretical models for flow of 100ml/min at 55°C

The absolute residential error values for BET model in all the cases of 55°C are very different as compared to the Langmuir and D-R models, which is also not matching with the experimental values. This proves the surface phenomenon and the porous nature of the material.

Table 4.8: Parametric values of Langmuir, BET, and D-R Isotherms at 55 C for ALC-SC-4:

| Flow Rate in ml/min | Langmuir parameters | | BET parameters | | D-R parameters | |
|---|---|---|---|---|---|---|
| | K | $V_m$ | C | $V_m$ | D | $V_0$ |
| 150 | 5.81 | 700 | 1.69 | 204 | .22 | 2153 |
| 125 | 3.17 | 900 | 1.46 | 167 | .24 | 2313 |
| 100 | 11.48 | 442 | 1.63 | 204 | .21 | 1706 |

Similarly. The experimental data at 60°C was used to model the adsorption kinetics using Langmuir,D-R and BET model.The Langmuir,D-R and BET parameters were calculated and depicted in Table 4.9 . The comparison between experimental values and parametric Langmuir, D-R and BET models for all the flow rates has been shown in Figure 4.17 to 4.19

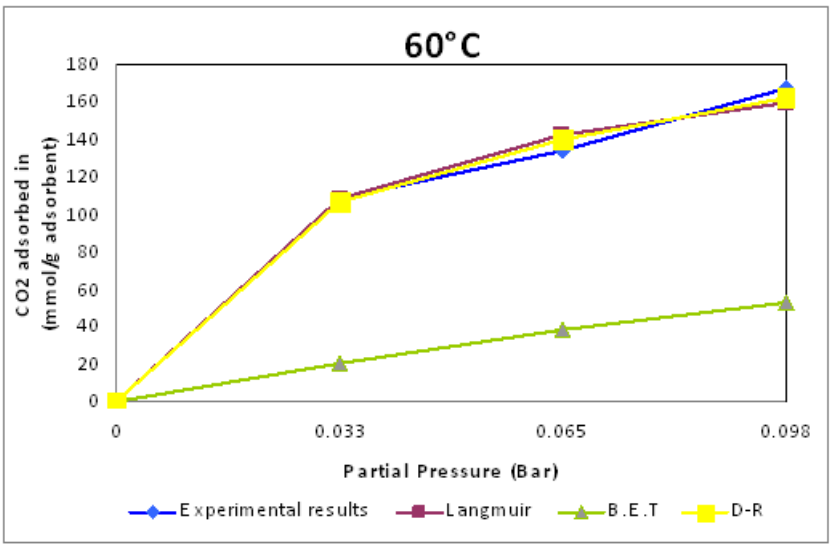


Figure 4.17: Comparison of experimental values with theoretical models for flow of 150ml/min at 60°C

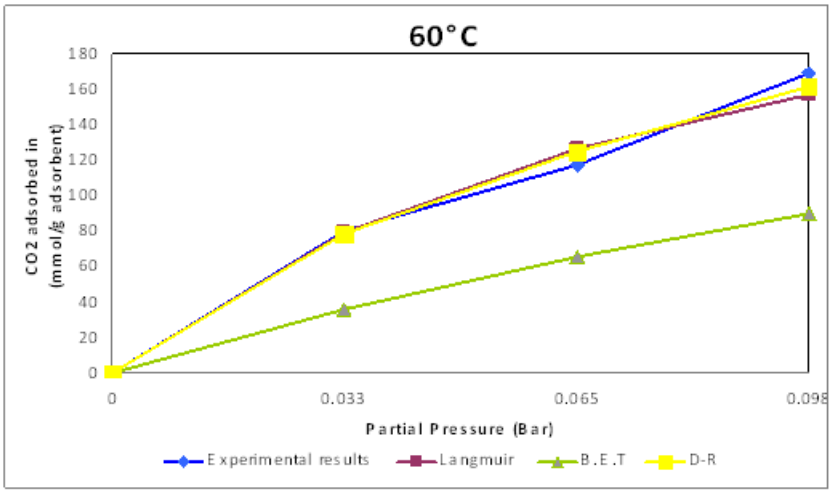


Figure 4.18: Comparison of experimental values with theoretical models for flow of 125ml/min at 60°C

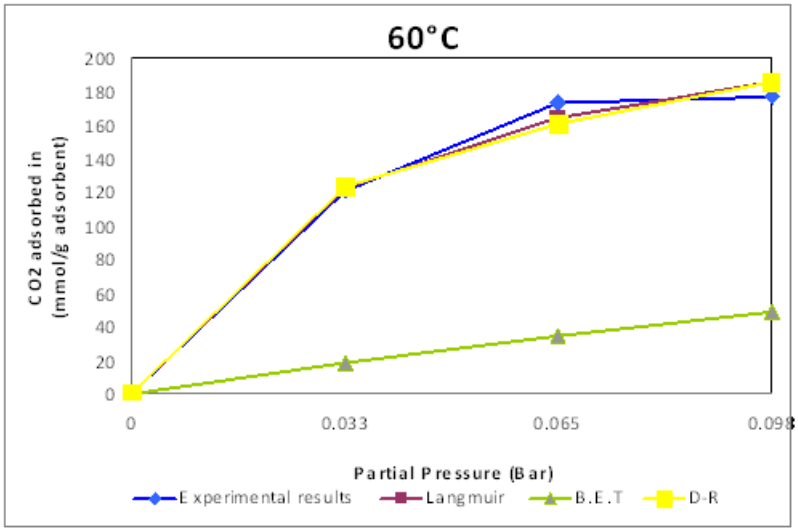


Figure 4.19: Comparison of experimental values with theoretical models for flow of 100ml/min at 60°C

Table 4.9: Parametric values of Langmuir, BET, and D-R Isotherms at 60°C for ALC-SC-4:

| Flow Rate in ml/min | Langmuir parameters | | BET parameters | | D-R parameters | |
|---|---|---|---|---|---|---|
| | K | $V_m$ | C | $V_m$ | D | $V_0$ |
| 150 | 32.39 | 210 | 2.91 | 149 | 0.16 | 518 |
| 125 | 10.51 | 310 | 1.55 | 137 | 0.22 | 1217 |
| 100 | 29.41 | 250 | 3.69 | 169 | 0.16 | 569 |

Also at the temperature of 65 °C experimental data was used to model the adsorption kinetics using Langmuir, BET, and D-R model. The Langmuir, BET, and D-R parameters were calculated and tabulated in Table 4.10 . The comparison between experimental values and parametric Langmuir, BET, and D-R models for the flow rates of 100,125 and 150 are shown in Figure 4.20 to 4.22 .

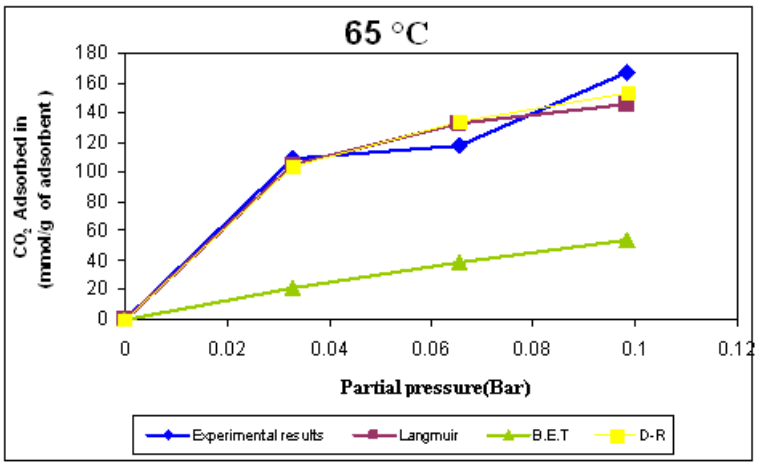


Figure 4.20: Comparison of experimental values with theoretical models for flow of 150ml/min at 65°C

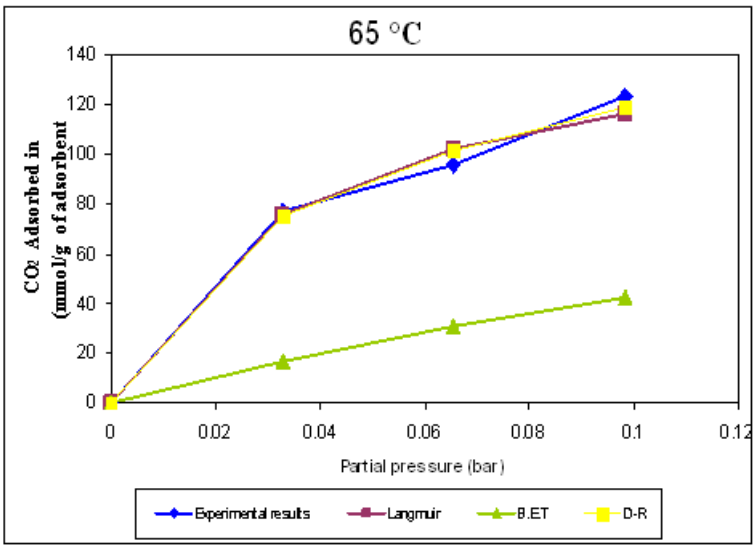


Figure 4.21: Comparison of experimental values with theoretical models for flow of 125ml/min at 65°C

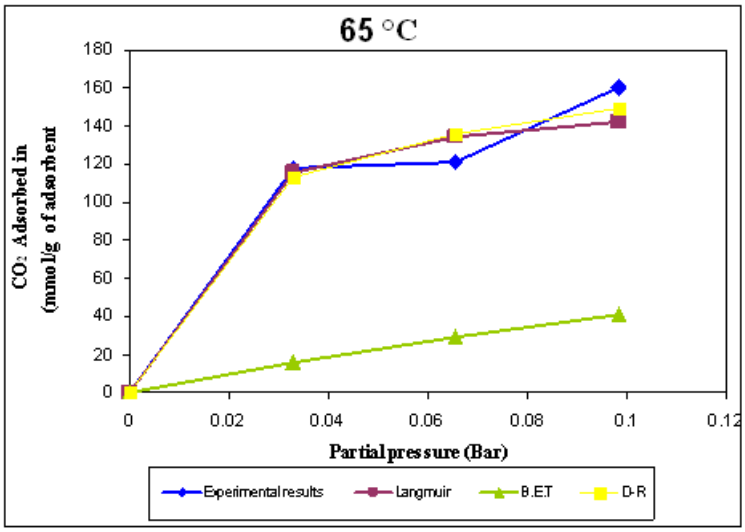


Figure 4.22: Comparison of experimental values with theoretical models for flow of 100ml/min at 65°C

Table 4.10: Parametric values of Langmuir, BET, and D-R Isotherms at 65°C for ALC-SC-4:

| Flow Rate in ml/min | Langmuir parameters | | BET parameters | | D-R parameters | |
|---|---|---|---|---|---|---|
| | K | $V_m$ | C | $V_m$ | D | $V_0$ |
| 150 | 42.74 | 180 | 2.69 | 143 | 0.61 | 450 |
| 125 | 28.13 | 158 | 2.58 | 108 | 0.17 | 425 |
| 100 | 80.13 | 160 | 3.68 | 143 | 0.13 | 322 |

### 4.1.6 Absolute residual error:

The percentage of Absolute Residual Error (ARE) was used to calculate the percentage deviation of the experimental results from the theoretical models discussed above. The percentage error was calculated using the following equation.

$$\%ARE = \frac{\sum_{i=1}^{j} abs(r_i)}{j} * 100$$

Where $r_i$ is the residual error calculated with the experimental value as the basis and j is the number of data points available for every sample. The percentage ARE values are shown in Table 4.11 . From the ARE results it can be observed that the BET model has highest residual error and Langmuir and D-A has lowest possible error. This justifies the fact that has been presented above as graphical comparison between experimental data and theoretical models. From the Table 4.11 the %ARE values for Langmuir and D-R are found to be comparatively very close. Moreover the values of Langmuir suggests that the Langmuir equation is capable to represent more perfectly the data obtained with% ARE not greater than 9% for all the flow rates at all the temperature that is 55, 60 and 65 °C which were under study.Langmuir approximation data for a flow rate of 125 ml/min are more accurate with a maximum error of not more than 9%.BET represents data with maximum error not more than 79%.

Table 4.11: Percentage absolute residual errors (%ARE) for Langmuir, BET, and D-R models:

| Flow Rate in ml/min | Temperature ℃ | % ARE Langmuir | % ARE BET | % ARE D-R |
|---|---|---|---|---|
| 150 | 55 | 7.25 | 53.83 | 7.95 |
| | 60 | 3.76 | 73.67 | 3.01 |
| | 65 | 9.04 | 71.54 | 8.92 |
| 125 | 55 | 8.63 | 44.64 | 9.01 |
| | 60 | 5.28 | 48.77 | 4.62 |
| | 65 | 4.71 | 70.64 | 3.77 |
| 150 | 55 | 5.17 | 50.02 | 4.44 |
| | 60 | 3.71 | 78.93 | 4.69 |
| | 65 | 8.01 | 78.88 | 7.48 |

### 4.1.7 Activation energy calculations:

To calculate the activation energy for the adsorption of $CO_2$, the rate of adsorption at three temperatures that is 55,60 and 65 have been used. Arrhenus equation is used for the calculation.

$$k = Ae^{\frac{-Ea}{RT}} \tag{4.1}$$

In short, the Arrhenius equation gives ‟The dependence of the rate constant k of chemical reactions on the temperature T (in absolute temperature, such as kelvins ) and activation energy Ea ″, as shown below

Rate constant values at 100 ml flow rate have been showed in the Table 4.12 Activation

Table 4.12: Activation energy at 100 ml/min flow

| Activation Energy Calculation (Flow Rate 100 cc/min) | | | | | |
|---|---|---|---|---|---|
| Flow Rate | Temp. ℃ | T | 1/T | K | ln(k) |
| 100 | 55 | 328 | 0.003 | 11.480 | 2.441 |
| 100 | 60 | 333 | 0.003 | 29.410 | 3.381 |
| 100 | 65 | 338 | 0.003 | 80.130 | 4.384 |

energy calculated from the above experiment is 42.7 Kcal/gmol, which is very similar to the reported in literature.

Similar studies with 125 and 150 ml/min flow rate was carried out to find out the

effect of contact time on the activation energy,results are tabulated in Table 4.13 and Table 4.14 respectively.

Activation energy Ea found for 125 ml/min flow was 48 Kcal/ gmol.

Table 4.13: Effect of temperature on rate of adsorption of $CO_2$ at 125 ml/min flow rate

| Activation Energy Calculation (Flow Rate 125 cc/min) | | | | | |
|---|---|---|---|---|---|
| Flow Rate | Temp. °C | T | 1/T | K | ln(k) |
| 125 | 55 | 328 | 0.003 | 3.170 | 1.154 |
| 125 | 60 | 333 | 0.003 | 10.510 | 2.352 |
| 125 | 65 | 338 | 0.003 | 28.130 | 3.337 |

Table 4.14 : Effect of temperature on rate of adsorption of CO2 at 150 ml/min flow rate Activation energy Ea found for 150 ml/min flow was 44 Kcal/ gmol.

Table 4.14: Effect of temperature on rate of adsorption of $CO_2$ at 150 ml/min flow rate

| Activation Energy Calculation (Flow Rate 150 cc/min) | | | | | |
|---|---|---|---|---|---|
| Flow Rate | Temp. °C | T | 1/T | K | ln(k) |
| 150 | 55 | 328 | 0.003 | 5.810 | 1.760 |
| 150 | 60 | 333 | 0.003 | 32.390 | 3.478 |
| 150 | 65 | 338 | 0.003 | 42.740 | 3.755 |

Lower activation energy i.e 42.7 Kcal/gmol observed with 100 ml/min flow rate would be most faverable conditions for the adsorption of $CO_2$ from the simulatd flue gas.

## 4.2 Sodium Carbonate deposited on Transition-Alumina:

### 4.2.1 Surface area analysis:

The surface area and pore volume of all samples prepared was measured using a static volumetric system (Micromeritics Instrument Corporation, USA, model ASAP 2020). The surface area was calculated using multi point Brunauer- Emmett and

Teller (BET) surface area method and the total pore volume was calculated from the amount of nitrogen adsorbed at relative pressure of 0.97.

The surface area and pore volume of the samples are given in the Table 4.15

Table 4.15: Surface area and Pore volume of the samples

| Sample name | Suface area ($m^2$/g) | Change in Surface Area ($m^2$/g) | Pore Volume ($cm^3$/g) | Change in Pore Volume ($cm^3$/g) |
|---|---|---|---|---|
| GAL-SC-0 | 321 | 0 | 0.397 | 0 |
| GAL-SC-1 | 278 | 43 | 0.368 | 0.029 |
| GAL-SC-2 | 262 | 59 | 0.351 | 0.046 |
| GAL-SC-3 | 191 | 130 | 0.328 | 0.069 |
| GAL-SC-4 | 190 | 131 | 0.344 | 0.053 |
| GAL-SC-5 | 185 | 136 | 0.308 | 0.089 |

Table 4.15 data infers the decrease of surface area and pore volume with increasing $Na_2CO_3$ loading, indicating the deposition of solute on the surface area available from all the pores, which in turn clog the pores and decrease the pore volume and surface area. The slight deviation in the case of 20 % loading it may be due to the experimental error.

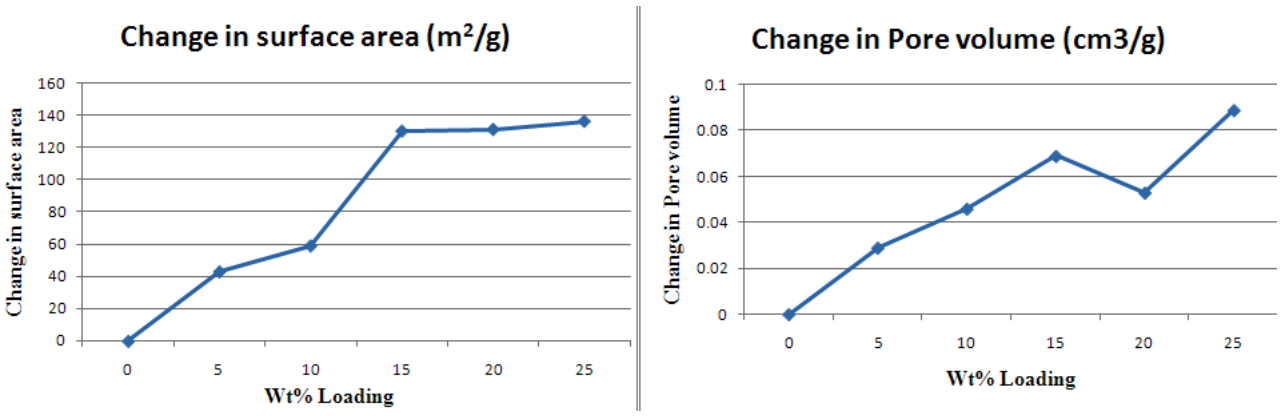


Figure 4.23: Change in surface area and pore volume of Transition Alumina

Figure 4.24 gives the pore size distribution it suggests that as alumina usually have pores in range of mesopores that is (20-500 Å). Maximum pores are in the range of 20-50 Å .

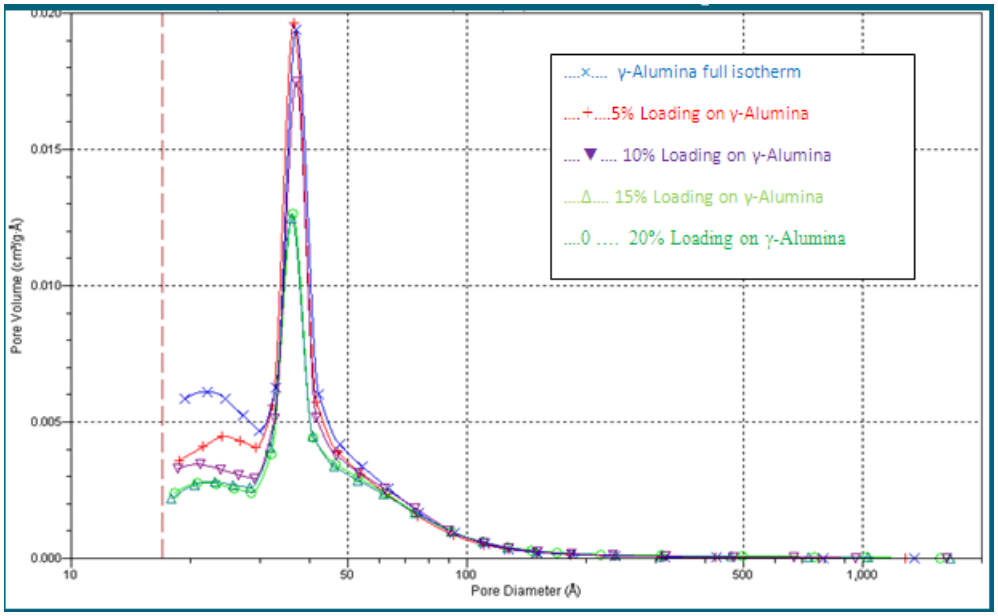


Figure 4.24: Pore size distribution of ALC

### 4.2.2 Effect of $Na_2CO_3$ loading :

The breakthrough curves for virgin and alkali-impregnated sample with different $CO_2$ concentration at 55 °C are shown in Figure 4.25 . There was an instrumental time lag of around 4 minutes after which $CO_2$ response was observed. $CO_2$ adsorption capacity has been used for screening and selecting the adsorbent for detail parametric study as per the DOE. The adsorption of $CO_2$ at close to atmospheric pressure requires chemical adsorbents with sodium carbonate impregnated over inorganic supports to increase the affinity towards $CO_2$ capture from flue gases. $CO_2$ adsorption capacities for all adsorbents are depicted in Figure 4.25 Overall, GAL-SC-4 (20% $Na_2CO_3$ on GAL) is found to have the highest $CO_2$ adsorption capacity at 55°C Table 4.16 .

$CO_2$ adsorption was increased with increase in carbonate loading up to 20 wt% and

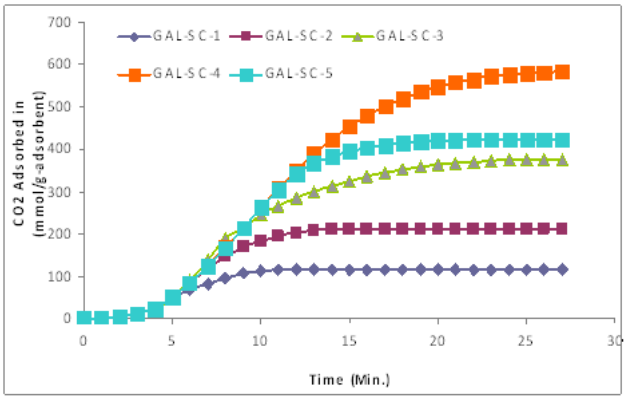


Figure 4.25: Comparison of $CO_2$ adsorption capacity of different adsorbents as a function of $Na_2CO_3$ loading at 8-vol% $CO_2$ concentration

Table 4.16: Adsorption capacities of selected samples of alkali-impregnated GAL with 8 vol% $CO_2$ in simulated flue gas

| Sample ID | $Na_2CO_3$ loading in wt% | $CO_2$ Adsorbed in (mmol/g of Adsorbent)at 50°C | $CO_2$ Adsorbed in (mg/g of Adsorbent) at 50°C |
|---|---|---|---|
| GAL-SC-0 | 0 | 0.0 | 0.0 |
| GAL-SC-1 | 5 | 116 | 5 |
| GAL-SC-2 | 10 | 211 | 9 |
| GAL-SC-3 | 15 | 376 | 17 |
| GAL-SC-4 | 20 | 583 | 26 |
| GAL-SC-5 | 25 | 423 | 19 |

then decreased at 25 wt% carbonate loading. If carbonate dispersion is the reason, the normalized values based on carbonate loading should decrease with increasing loading. The above trend followed up to 15-wt%, whereas at 20 wt% the uptake increased. To check the reproducibility of the above results, the experiments were performed three times under identical conditions. Results are reproducible with standard deviation of less than 5% as shown in Figure 4.26 and Reproducibility of $CO_2$ adsorption experiments shows very good level of confidence i.e. 95%. Table 4.17 .

As adsorption was highest and the result was also reproducible to an accuracy level of around 95% so GAL-SC-4 (20% $Na_2CO_3$ on GAL) was selected for detail parametric

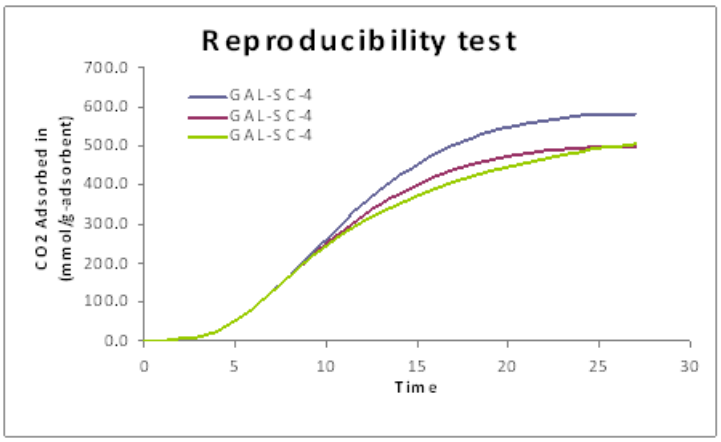


Figure 4.26: Reproducibility of GAL-SC-4 under similar condition

Table 4.17: Adsorption capacities of selected samples of alkali-impregnated GAL with 8 vol% $CO_2$ in simulated flue gas

| Temperature | Sample name | $Na_2CO_3$ loading | $CO_2$ Adsorbed in(mg/gm of adsorbent) | $CO_2$ Adsorbed in(mmol/gm of adsorbent) |
|---|---|---|---|---|
| 55°C | GAL-SC-4 | 20% | 26 | 583 |
| 55°C | GAL-SC-4 | 20% | 22 | 490 |
| 55°C | GAL-SC-4 | 20% | 24 | 540 |

study under DOE.

For the selection of temperature on which the DOE would be based we did experiment on GAL-SC-4 at different temperatures (45, 50, 55, 60, and 65 °C) keeping all the other conditions same. From the results as shown in Figure 4.27 we can see that the adsorption of $CO_2$ increased till 50 °C and then their was a fall in the adsorption for 45 °C so for DOE we have chosen the three temperature as 50, 55, and 60 °C.

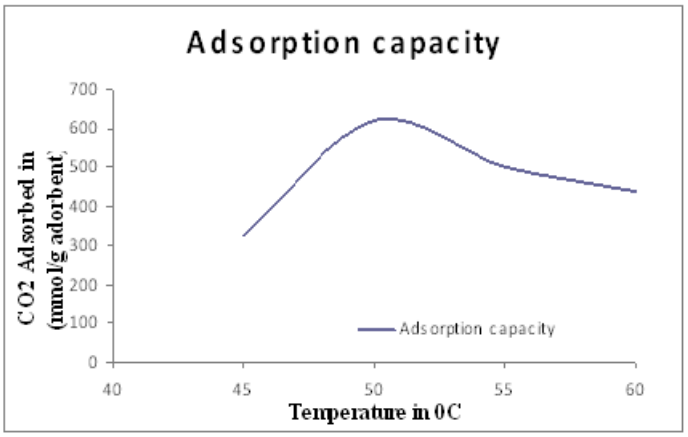


Figure 4.27: Adsorption of $CO_2$ by GAL-SC-4 under similar condition at different temperatures

### 4.2.3 Studies to optimize process parameters:

GAL-SC-4 sample was chosen for the process parameter optimization study. In this study the effect of process parameters, we have considered were 3 process variables at 3 levels which are shown in Table 4.18

Table 4.18: Levelsof DOE for GAL-SC-4

| Process parameter | Temperature | $CO_2$ | Flow Rate(ml/min) |
|---|---|---|---|
| Level-1 | 50 | 3 | 100 |
| Level-2 | 55 | 6 | 125 |
| Level-3 | 60 | 9 | 125 |

Statistical designing of experiments (DOE) were prepared by using Minitab software. Objective of the design of experiment is to provide correlations and interactions between various parameters. Simulated flue gas with 3, 6, 9 vol% $CO_2$ with constant i.e, 2.5 vol% $H_2O$ and balance $N_2$. Flow rates varied during the study were 100, 125 and 150 ml/min. The mixture was chemically adsorbed by the supported $Na_2CO_3$ at 50 - 60 °C temperature, which converts the carbonate to bicarbonate ($NaHCO_3$)

of sodium. Adsorbent was then regenerated at elevated temperature of 120 °C and to produce concentrated $CO_2$ stream from the flue gas.

### 4.2.4 Effect of temperature :

Effect of temperature was studied at different flow rates with the same $CO_2$ concentration in simulated flue gases. Temperature was varied in a step of 5 °C starting from 50°C.

Figure 4.28 shows the results of $CO_2$ adsorption from flue gas containing 3% $CO_2$ .During the above experiment flue gas flow rate of 150ml/min was used. As per the experimental design temperature was varied. It has been observed that there was a negligible effect of temperature at low concentration of $CO_2$ in simulated flue gas stream. Reason for the above may be due to the lower partial pressure of $CO_2$ in the flue gas, making the population of active sites excess then the adsorbate.

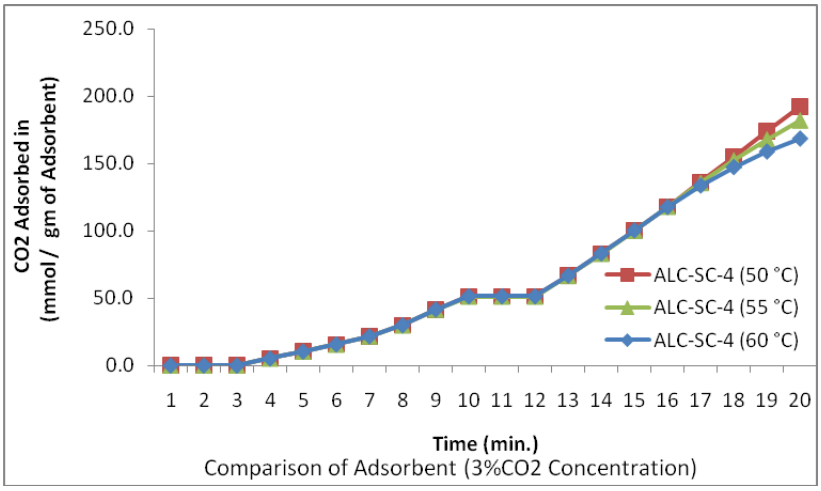


Figure 4.28: Comparision of adsorbent at 150 ml/min flow rate and 3% CO2 concentration

The similar observation was drawn in the case of 125 ml/min which was shown in the Figure 4.29 at different temperatures of 50, 55, 60 °C. It has been observed that there was negligible effect of temperature with low concentration of $CO_2$ in simulated flue

gas stream, which may be due to the lower partial pressure of $CO_2$ in the flue gas, making the population of active sites excess then the adsorbate.

The same trend was also seen when the flow was 100 ml/min the reason are the

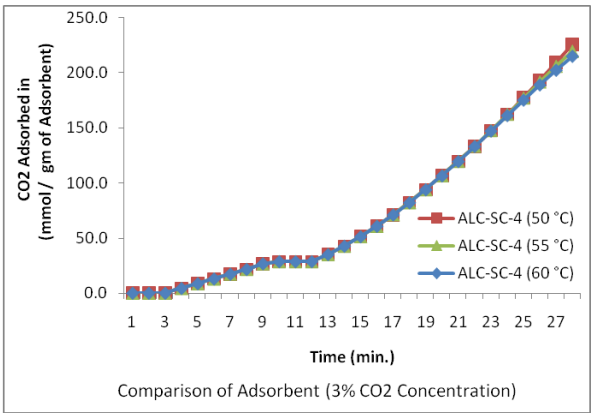


Figure 4.29: Comparision of adsorbent at 125 ml/min flow rate and 3% CO2 concentration

same as that were for the two previous simulated flows of 150 and 125 ml/min. The result is shown in Figure 4.30

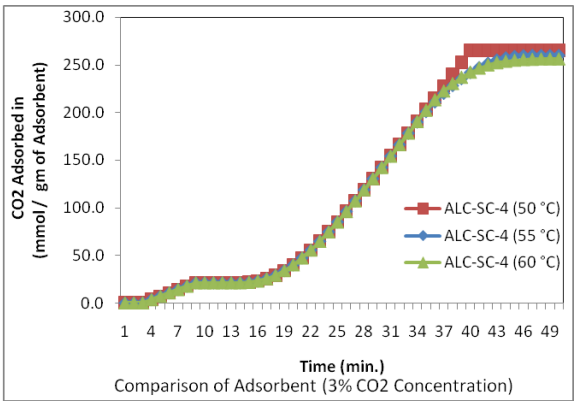


Figure 4.30: Comparision of adsorbent at 100 ml/min flow rate and 3% CO2 concentration

To find the optimized concentration of $CO_2$, the concentration was increased. At 6 % concentration of $CO_2$ in the simulated flue gas Figure 4.31 , which shows the variation in the adsorption of $CO_2$ at total flow rate of 150 ml/min at different temperatures 50, 55, 60 °C. It has been observed that as the temperature increases the adsorption decreases from 55°C to 60°C which is in accordance with the literature. The adsorption decreases drastically when the temperature was increased by 5 °C. The adsorption rate was not changed much when the temperature was further raised to 60 °C, which may be due to desorption of $CO_2$.

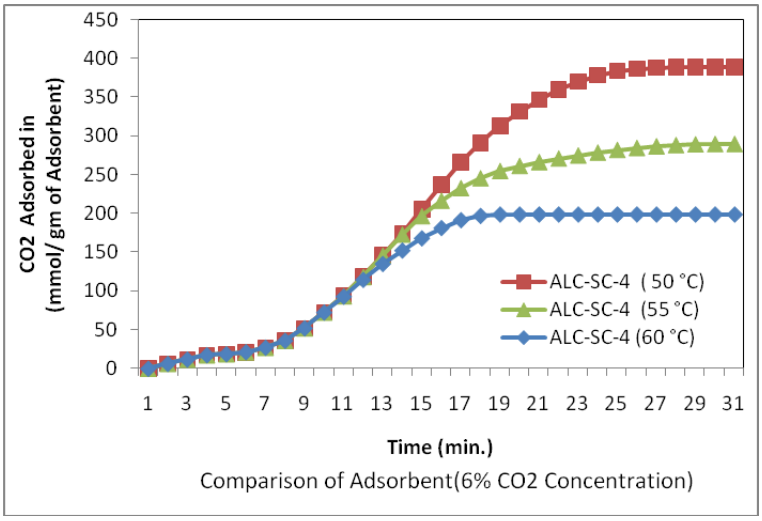


Figure 4.31: Comparison of adsorbent at 150 ml/min flow rate and 6% CO2 concentration

The Figure 4.32 depicts the adsorption of $CO_2$ at total flow rate of 125ml/min at different temperatures of 50 - 60°C. The same trend was observed in case of 100 ml/min flow but with slight difference, the $CO_2$ adsorption decreases with increase in temperature. There was continuous drop in the adsorption of $CO_2$ for the increase in temperatures; this may be due to the high contact time between the $CO_2$ and adsorbent.

Slight difference in adsorption pattern was observed in case of 100 ml/min flow rate Figure 4.33 . The adsorption was increased in initial stage of experiment at 50 °C as

a function of time (9 - 15 min) afterwards attaints the maximum adsorption as in the case of 60 °C. This may be due the inconsistency in bed packing.

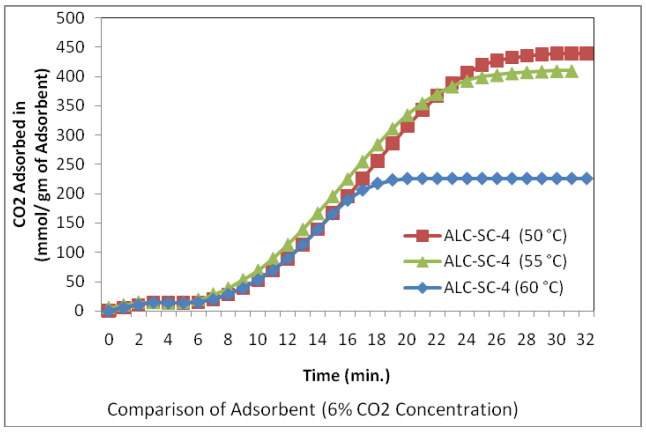


Figure 4.32: Comparision of adsorbent at 125 ml/min flow rate and 6% $CO_2$ concentration

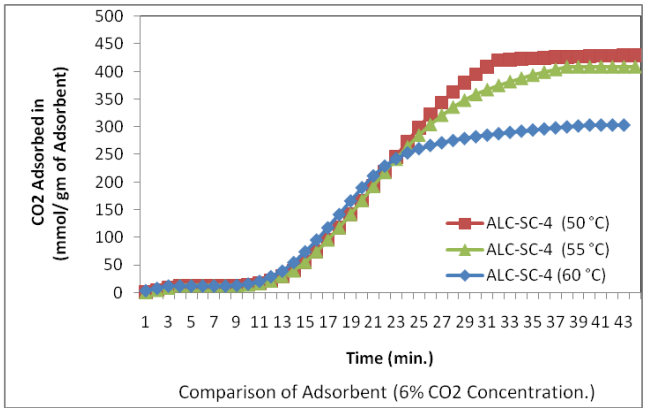


Figure 4.33: Comparison of adsorbent at 100 ml/min flow rate and 6% $CO_2$ concentration

Further the concentration of $CO_2$ was increased to 9 % to find the maximum adsorption for $CO_2$ at different temperatures Figure 4.34 . At 9 % $CO_2$ concentration at 150 ml/min the adsorption was 531 mmol/g as compared to the 6 % $CO_2$ concentration (389 mmol/g) at 50 °C, this is due to the availability of $CO_2$. The similar trend was observed when the temperature was increased from 55 to 60 °C, which is because of the adsorption-desorption equilibrium.

Figure 4.35 and 4.36 shows the adsorption pattern for $CO_2$ at 125 and 100 ml/min

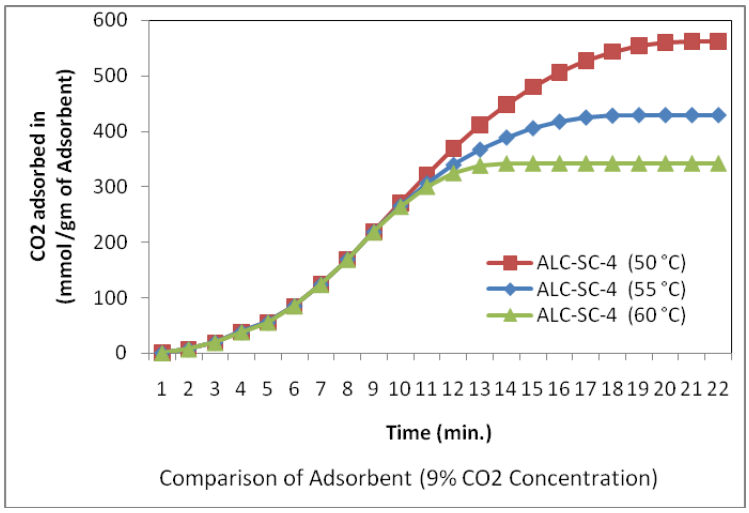


Figure 4.34: Comparision of adsorbent at 150 ml/min flow rate and 9% CO2 concentration

flow rate respectively at 9 % concentration. The adsorption goes on decreasing as function of temperature.

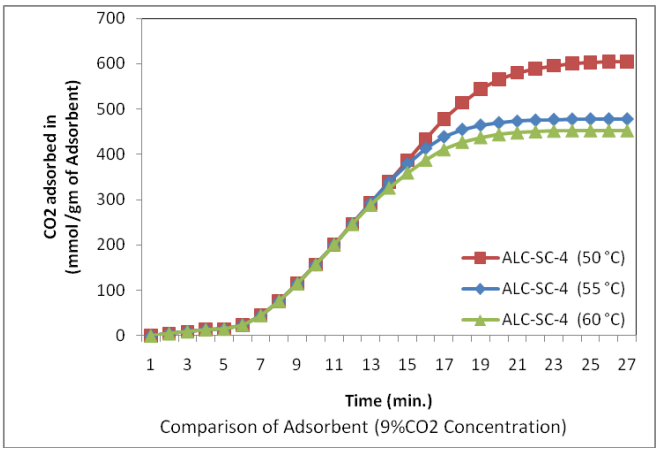


Figure 4.35: Comparision of adsorbent at 125 ml/min flow rate and 9% CO2 concentration

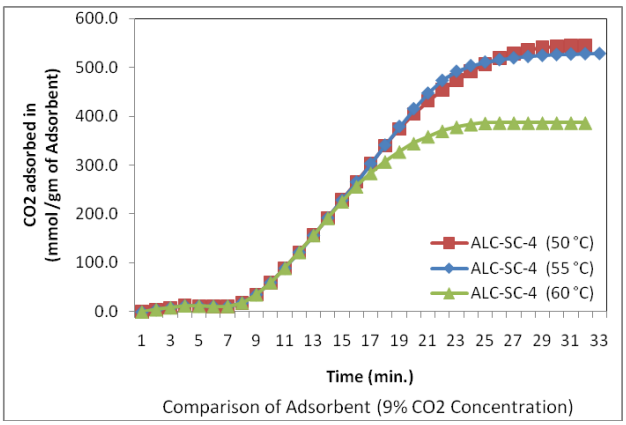


Figure 4.36: Comparision of adsorbent at 100 ml/min flow rate and 9% CO2 concentration

The effects of different temperatures and $CO_2$ concentrations are given in Table 4.19 . It is very much clear for the values that the adsorption increases with increase in concentration and decreases with increase in temperature. This is due to the high contact time and desorption phenomenon at elevated concentration and temperature. It has been observed that there was a negligible effect of temperature with low concentration of $CO_2$ in simulated flue gas stream.

Same trend was seen when the flow rate was 125 ml/min and 100ml/min as shown

Table 4.19: Adsorption of CO2 at 150ml/min at different temperatures

| Carbon dioxide adsorbed in mmol/g of adsorbent | | | |
|---|---|---|---|
| Temperature°C | 9 volume % $CO_2$ | 6 volume % $CO_2$ | 3 volume % $CO_2$ |
| 50 | 562 | 389 | 192 |
| 55 | 429 | 290 | 182 |
| 60 | 342 | 198 | 168 |

in Table 4.20 and Table 4.21 respectively.

Table 4.20: Adsorption of $CO_2$ at 125ml/min at different temperatures

| Carbon dioxide adsorbed in mmol/g of adsorbent | | | |
|---|---|---|---|
| Temperature°C | 9 volume % $CO_2$ | 6 volume % $CO_2$ | 3 volume % $CO_2$ |
| 50 | 605 | 438 | 226 |
| 55 | 478 | 409 | 219 |
| 60 | 452 | 226 | 215 |

Table 4.21: Adsorption of $CO_2$ at 100ml/min at different temperatures

| Carbon dioxide adsorbed in mmol/g of adsorbent | | | |
|---|---|---|---|
| Temperature°C | 9 volume % $CO_2$ | 6 volume % $CO_2$ | 3 volume % $CO_2$ |
| 50 | 545 | 430 | 265 |
| 55 | 529 | 408 | 256 |
| 60 | 387 | 303 | 260 |

### 4.2.5 Isotherms for GAL-SC-4:

Various isotherms for adsorption of gases on solids have been analyzed at different temperatures under which the experiments were carried out that is at 50 °C, 55 °C, and 60 °C using different approaches such as Langmuir theory, BET theory, Polanyi Potential theory.

The experimental data at 50°C was used to model the adsorption kinetics using Langmuir model. The Langmuir parameters were calculated and given below Table 4.22 . The comparison between experimental values and parametric Langmuir, D-R and BET isotherm models for all the flow rates has been shown in Figure 4.37 to Figure 4.39 at all flow rates. From the graphs it is very much clear that Langmuir model is exactly fitting with the experimental data, so hence forth Langmuir isotherm modeling curves are used to calculate the activation energy for $CO_2$.

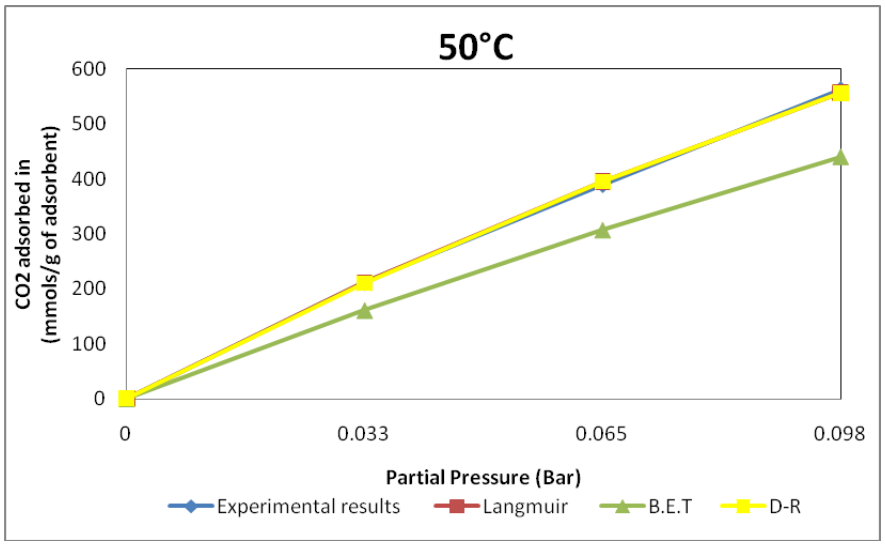


Figure 4.37: Comparison of experimental values with theoretical models for flow of 150ml/min at 50°C

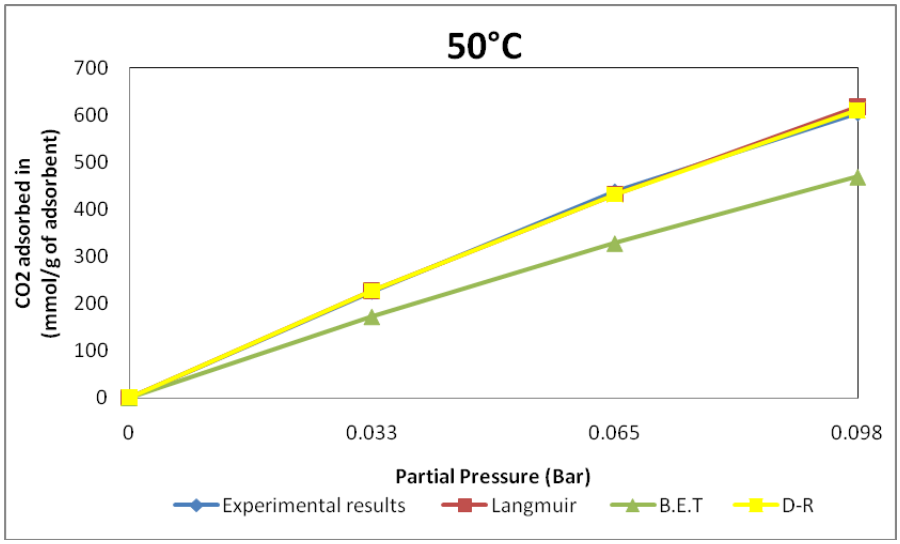


Figure 4.38: Comparison of experimental values with theoretical models for flow of 125ml/min at 50°C

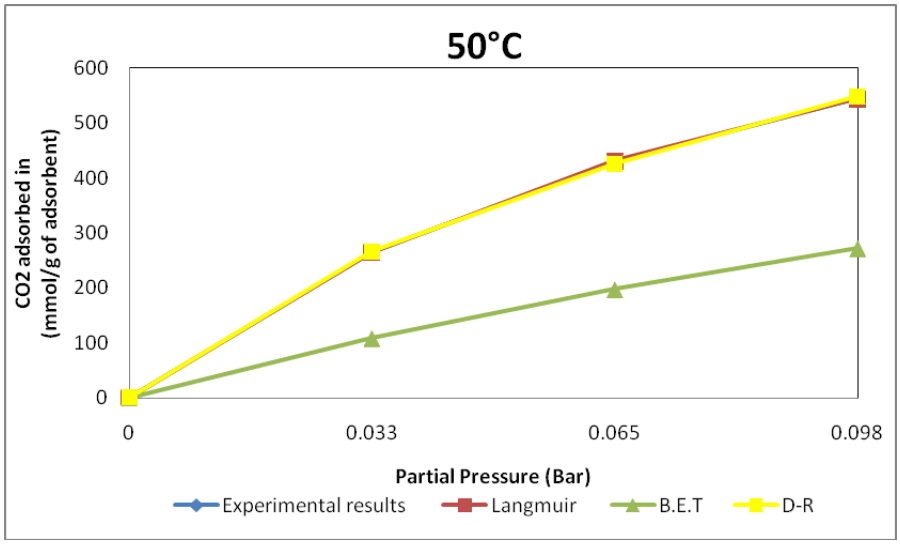


Figure 4.39: Comparison of experimental values with theoretical models for flow of 100ml/min at 50°C

Table 4.22: Parametric values of Langmuir, BET, and D-R Isotherms at 50 °C for GAL-SC-4:

| Flow Rate in ml/min | Langmuir parameters | | BET parameters | | D-R parameters | |
|---|---|---|---|---|---|---|
| | K | $V_m$ | C | $V_m$ | D | $V_0$ |
| 150 | 2.3 | 3021 | 1.15 | 435 | 0.25 | 8376 |
| 125 | 1.67 | 4380 | 1.17 | 476 | 0.25 | 9562 |
| 100 | 9.14 | 1150 | 1.69 | 455 | 0.21 | 4112 |

Similarly. The experimental data at 55°C was used to model the adsorption kinetics using Langmuir, BET and D-R models. The Langmuir, BET and D-R parameters were calculated the data has been given below Table 4.23 . Comparisons of experimental data at 55C and flow rate of 150, 125, and 100 ml/min for Langmuir, BET, and D-R are shown in Figure 4.40 to 4.42 .

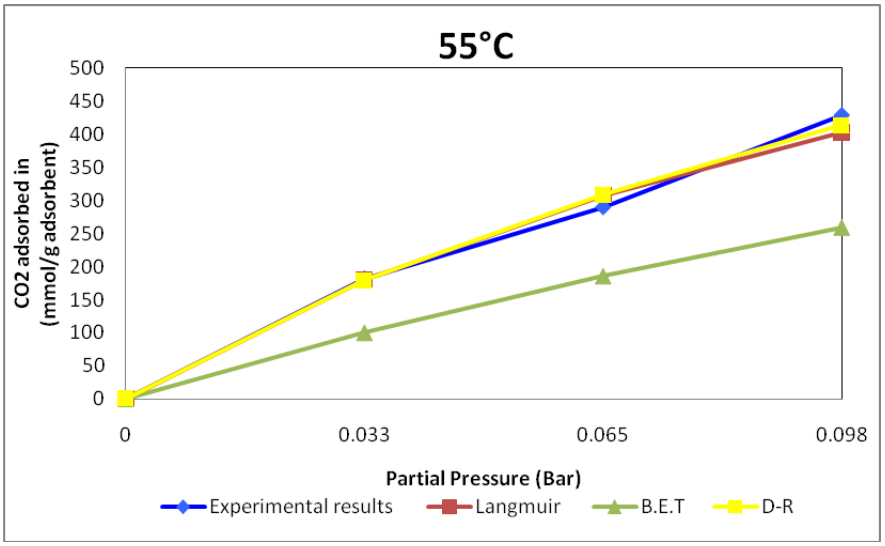


Figure 4.40: Comparison of experimental values with theoretical models for flow of 150ml/min at 55°C

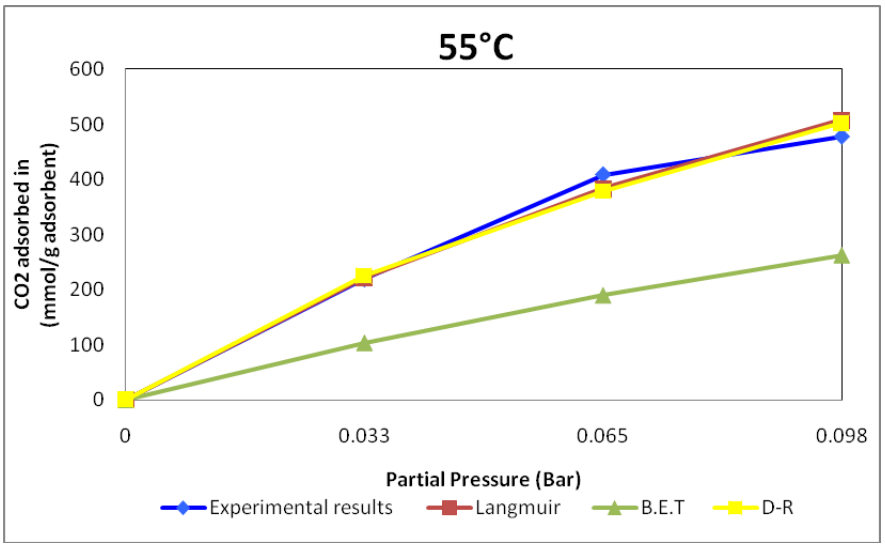


Figure 4.41: Comparison of experimental values with theoretical models for flow of 125ml/min at 55°C

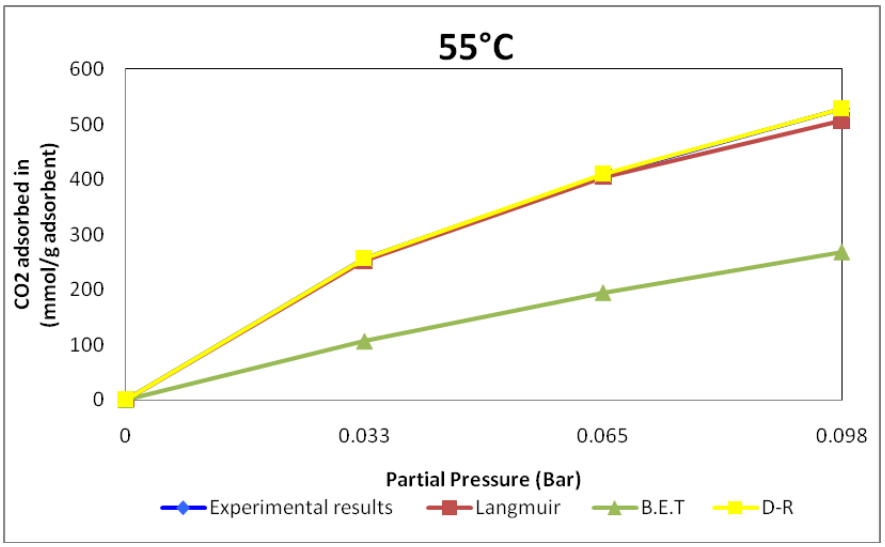


Figure 4.42: Comparison of experimental values with theoretical models for flow of 100ml/min at 55°C

Table 4.23: Parametric values of Langmuir, BET, and D-R Isotherms at 55°C for GAL-SC-4:

| Flow Rate in ml/min | Langmuir parameters | | BET parameters | | D-R parameters | |
|---|---|---|---|---|---|---|
| | K | $V_m$ | C | $V_m$ | D | $V_0$ |
| 150 | 6.31 | 1053 | 1.36 | 333 | 0.23 | 4271 |
| 125 | 5.51 | 1446 | 1.56 | 400 | 0.23 | 4691 |
| 100 | 9.89 | 1029 | 1.64 | 435 | 0.21 | 3964 |

Similarly . The experimental data at 60°C was used to model the adsorption kinetics using Langmuir, D-R and BET model. The Langmuir, D-R and BET parameters were calculated the data has been given below Table 4.24 . Comparisons of experimental data at 60°C and flow rate of 150, 125, and 100 ml/min to all the isotherm models such as Langmuir, BET, and D-R are shown in Figure 4.43 to 4.45 .

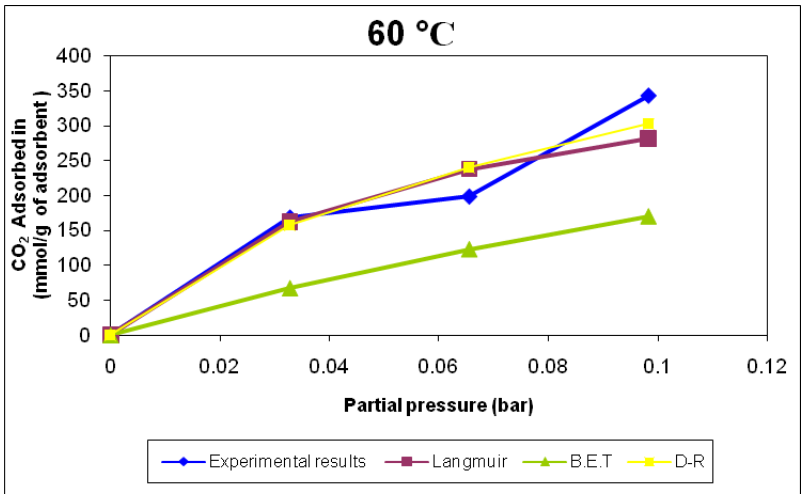


Figure 4.43: Comparison of experimental values with theoretical models for flow of 150ml/min at 60°C

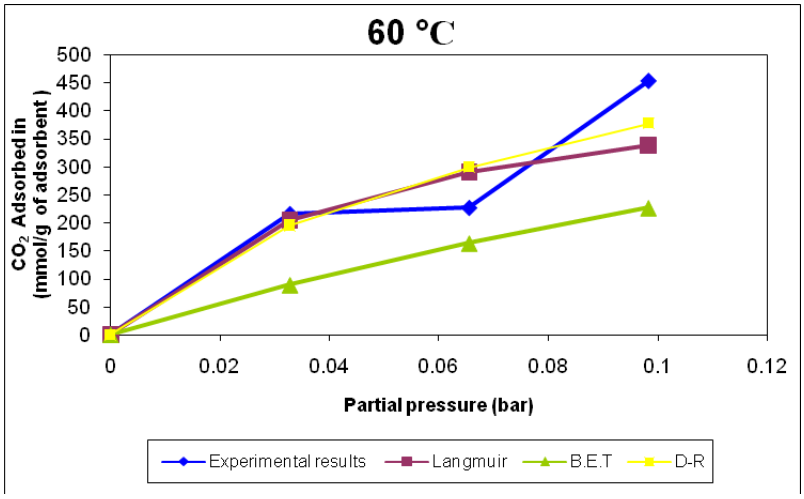


Figure 4.44: Comparison of experimental values with theoretical models for flow of 125ml/min at 60°C

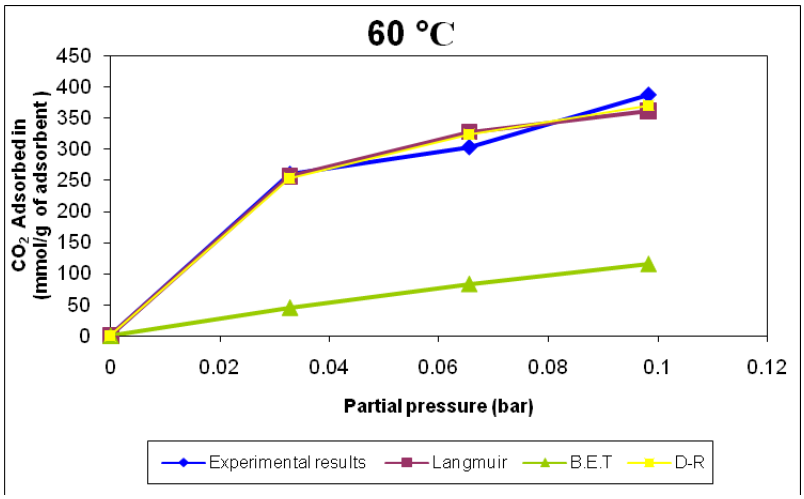


Figure 4.45: Comparison of experimental values with theoretical models for flow of 100ml/min at 60°C

Table 4.24: Parametric values of Langmuir, BET, and D-R Isotherms at 60°C for GAL-SC-4:

| Flow Rate in ml/min | Langmuir parameters | | BET parameters | | D-R parameters | |
|---|---|---|---|---|---|---|
| | K | $V_m$ | C | $V_m$ | D | $V_0$ |
| 150 | 17.58 | 444 | 1.58 | 263 | 0.20 | 1859 |
| 125 | 20.71 | 505 | 1.48 | 323 | 0.21 | 2361 |
| 100 | 39.31 | 455 | 3.00 | 333 | 0.16 | 1058 |

### 4.2.6 Absolute residual error:

The percentage of Absolute Residual Error (ARE) was used to calculate the percentage deviation of the experimental results from the theoretical models discussed above. The percentage error was calculated using the following equation.

$$\%ARE = \frac{\sum_{i=1}^{j} abs(r_i)}{j} * 100$$

Where $r_i$ is the residual error calculated with the experimental value as the basis and j is the number of data points available for every sample. The percentage ARE values

Table 4.25: Percentage absolute residual errors (%ARE) for Langmuir, BET, and D-R models:

| Flow Rate in ml/min | Temperature ℃ | % ARE Langmuir | % ARE BET | % ARE D-R |
|---|---|---|---|---|
| 150 | 50 | 0.96 | 22.36 | 1.00 |
| | 55 | 4.39 | 40.16 | 3.86 |
| | 60 | 13.74 | 49.48 | 13.14 |
| 125 | 50 | 1.31 | 23.72 | 1.00 |
| | 55 | 4.47 | 50.55 | 5.09 |
| | 60 | 9.60 | 45.49 | 19.42 |
| 100 | 0.12 | 54.51 | 0.68 | |
| | 55 | 2.22 | 53.28 | 0.20 |
| | 60 | 5.43 | 75.25 | 4.61 |

are shown in Table 4.25 . From the ARE results it can be observed that the BET model has highest residual error and Langmuir and D-A has lowest possible error. This justifies the fact that has been presented above as graphical comparison between experimental data and theoretical models. From the Table 4.25 , the %ARE values for

Langmuir and D-R are found to be comparatively very close. For all the temperatures under all flows %ARE values of both D-R and Langmuir models are relatively close to each other. Moreover the values of Langmuir suggests that the Langmuir equation is capable to represent more perfectly the data compared to other models studied with% ARE not greater than 14% for all the flow rates at all the temperature that is 50, 55 and 60 °C which were under study. Langmuir approximation data for a flow rate of 100 ml/min are the most accurate with a maximum error of not more than 6%.BET represents data with maximum error not more than 76%. At lower temperature that is at 50 °C for all the flow rate under study the %ARE in the case of Langmuir and D-R model is not more than 2%.

### 4.2.7 Activation energy calculations:

To calculate the activation energy for the adsorption of $CO_2$, the rate of adsorption at three temperatures that is 50,55 and 60 °C have been used. Arrhenus equation is used for the calculation.

$$k = Ae^{\frac{-E_a}{RT}} \tag{4.2}$$

In short, the Arrhenius equation gives ‟The dependence of the rate constant k of chemical reactions on the temperature T (in absolute temperature, such as kelvins ) and activation energy Ea ″, as shown below

Rate constant values at 100 ml flow rate have been showed in the Table 4.26 Activation

Table 4.26: Activation energy at 100 ml/min flow

| Activation Energy Calculation (Flow Rate 100 cc/min) | | | | | |
|---|---|---|---|---|---|
| Flow Rate | Temp. °C | T | 1/T | K | ln(k) |
| 100 | 50 | 323 | 0.003 | 9.14 | 2.2213 |
| 100 | 55 | 328 | 0.003 | 9.89 | 2.292 |
| 100 | 60 | 333 | 0.003 | 39.31 | 3.671 |

energy calculated from the above experiment is 31.07 Kcal/gmol, which is very similar to the reported in literature.

Similar studies with 125 and 150 ml/min flow rate was carried out to find out the effect of contact time on the activation energy,results are tabulated in Table 4.27 and Table 4.28 respectively.

Activation energy Ea found for 125 ml/min flow was 54 Kcal/ gmol.

Table 4.27: Effect of temperature on rate of adsorption of CO2 at 125 ml/min flow rate

| Activation Energy Calculation (Flow Rate 125 cc/min) | | | | | |
|---|---|---|---|---|---|
| Flow Rate | Temp. °C | T | 1/T | K | ln(k) |
| 125 | 50 | 323 | 0.003 | 1.670 | 0.513 |
| 125 | 55 | 328 | 0.003 | 5.510 | 1.707 |
| 125 | 60 | 333 | 0.003 | 20.710 | 3.031 |

Table 4.28 : Effect of temperature on rate of adsorption of $CO_2$ at 150 ml/min flow rate Activation energy Ea found for 150 ml/min flow was 43 Kcal/gmol.

Table 4.28: Effect of temperature on rate of adsorption of CO2 at 150 ml/min flow rate

| Activation Energy Calculation (Flow Rate 150 cc/min) | | | | | |
|---|---|---|---|---|---|
| Flow Rate | Temp. °C | T | 1/T | K | ln(k) |
| 150 | 50 | 328 | 0.003 | 2.3 | 0.833 |
| 150 | 55 | 333 | 0.003 | 6.310 | 1.842 |
| 150 | 60 | 338 | 0.003 | 17.580 | 2.867 |

Lower activation energy i.e 42.7 Kcal/gmol observed with 100 ml/min flow rate would be most favorable conditions for the adsorption of CO2 from the simulated flue gas.

# Chapter 5

# Conclusion

Aluminas are abundant in nature and the thermal, physical and chemical stability of alumina is very high. The basic nature of alumina can be utilized for the adsorption-desorption studies for $CO_2$, which is one of the industrial concern as an environmental point of view. The porosity of alumina can be very well utilized for the same. Sodium carbonate ($Na_2CO_3$) impregnated on alumina and clay (ALC) and transition-Alumina can be used as an adsorbent to remove carbon dioxide from flue gases as it possess high adsorption capacity for carbon dioxide adsorption. Aluminas are modified using different percentage of metal loading of Sodium carbonate. The maximum (251 mmol/g) adsorption for ALC-SC-4 was observed when the temperature was 55 °C, flow rate 100 ml/min and the concentration was 9 %. Sodium carbonate ($Na_2CO_3$) impregnated on transition -Alumina has adsorption capacity of 605 mmol/g at 125 ml/min flow rate, 50 °C, 9 % concentration for carbon dioxide at atmospheric pressure for flue gas. The regeneration of alumina at higher temperature doesn't affect the nature of the materials, so these materials can be used for industrial application. It is possible to enhance the carbon dioxide adsorption capacities by further modifying surface functional group and also by using support having high surface area.

Different theoretical models were applied to the experimental adsorption data to get nature of adsorption like monolayered or multilayered. The models applied were

Langmuir, BET, Dubinin- Radushkevich. Langmuir model was found to be most consistent with the experimental data with the value of correlation coefficient $R^2 >$ 95%. Further, the activation energy was calculated using the best fitted model.

Thus transition alumina supports with narrow pore size distribution and high pore volume will be highly desirable for industrial purpose.

Forward path for the project can be detail kinetic study at very low or high reaction parameters. Different metal salts, supports having high surface area, surface modifications for the existing adsorbent. The data generated by DOE will be utilized for developing surface response model and unique algorithms to know the adsorption capacity of adsorbent at various conditions which will be used to design future process.

# References


[1] Aaron D, Tsouris C. Separation of CO2 from flue gas: A review. Separation Science and Technology 2005;40(1-3):321-348.

[2] J.D. Figueroa TF, S. Plasynski, H. McIlvried, R.D. Srivastava, . Advances in CO2 capture technology - the US Department of energy's carbon sequestration program,. International Journal of Greenhouse Gas Control 2008;2 (1):9-20.

[3] Eliane Blomen CH, Filip Neele, . Capture technologies: Improvements and Promising Developments, . Energy Procedia 2009;1:1505-1512.

[4] Klara SM, Srivastava, R.D., McIlvried, H.G.,Integrated collaborative technology development program for CO2 sequestration in geologic formations-United States Department of Energy R& D. Energy Conv Manage 2003.;44, :2699-2712.

[5] Amit G, P.R. Shukla;. Coal and energy security for India: Role of carbon dioxide (CO2) capture and storage (CCS);. Energy 2009;34:1032-1041.

[6] Yang H, Xu Z, Fan M, Gupta R, Slimane RB, Bland AE, et al. Progress in carbon dioxide separation and capture: A review. Journal of Environmental Sciences 2008;20(1):14-27.

[7] National Aeronautics and Space Administration, ¨Global Warming ″, The Earth Science Enterprise Series, June 2002, Goddard Space Flight Center, Greenbelt, Maryland 20771.

[8] Marquita k. hill, ¨Understanding environmental pollution ″, Cambridge university press, pp 123-137.

[9] Arthur B. Robinson, Salline L. Baliunas, ¨Environmental effects of increased atmospheric carbon dioxide ″, Oregon institute of science and medicine, (Available online at http://www.oism.org./pproject/review.pdf).

[10] John Marion, Nsakala ya Nsakala, ¨Controlling power plant CO2 emissions: A long range view ″, ALSTOM Power Plant Laboratories.

[11] Jiri V.S, Frank G, Nicholas G, Georgios P, Liam M. CO2 capture for refineries, a practical approach. Energy Procedia 1 2009 179-185.

[12] ¨Carbon sequestration, technology roadmap and program plan-2004 ″, April 2004, U.S. Department of energy, National energy technology laboratory. Available online at http://www.fossil.energy.gov/programs/sequestration/publications/programplans/2004/Seq 29-04.pdf).

[13] John Gale, ¨Overview of CO2 emission sources, potential, transport and geographical distribution of storage possibilities ″, workshop on carbon dioxide capture and storage proceedings, Regina, Canada, 18-21 November, 2002.

[14] Robert B. Bacastow, Richard K. Dewey, ¨Effectiveness of carbon dioxide sequestration in the post industrial ocean″Energy Convers. Mgmt vol. 37, Nos 6-8, pp. 1079-1086, 1996.

[15] N. A. Al-Baghli, S. A. Pruess, V. F. Yesavage , M. S. Selim, ¨A rate-based model for the design of gas absorbers for the removal of CO2 and H2S using aqueous solutions of MEA and DEA″, Fluid phase equilibria, 185 (2001), pp 31-43.

[16] Axel Meisen and Xiaoshan Shuai, ¨Research and development issues in CO2 capture″, Energy conversion management, volume 38, suppl., pp S37-S42, 1997.

[17] Sam Wong and Rob Bioletti, ¨Carbon dioxide separation technologies″, Carbon and energy management, Albetra research council Edmonton, Canada.

[18] J. Tim Cullinane, Gary T. Rochelle, ¨Carbon dioxide absorption with aqueous potassium carbonate promoted by piperazine″, Chemical Engineering Science, 59 (2004), pp 3619 - 3630.

[19] M. R. Rahimpour, A .Z. Kashkooli, ¨Enhanced carbon dioxide removal by promoted hot potassium carbonate in a split-flow absorber″, Chemical Engineering and Processing, 43 (2004), pp 857-865

[20] B. P. Mandala, M. Guhab, A. K. Biswasb, S. S. Bandyopadhyaya, ¨Removal of carbon dioxide by absorption in mixed amines: modeling of absorption in aqueous MDEA/MEA and AMP/MEA solutions″, Chemical Engineering Science, 56 (2001), pp 6217-6224.

[21] Yong-Fa Diao, Xian-Yu Zheng, Bo-Shu He, Chang-He Chen, ¨Experimental study on capturing CO2 greenhouse gas by ammonia scrubbing″, Energy Conversion and Management, 45 (2004), pp 2283-2296.

[22] An Chin Yeh, Hsunling BaiU, ¨Comparison of ammonia and monoethanolamine solvents to reduce CO2 greenhouse gas emissions″, The Science of the Total Environment, 228 (1999), pp 121-133.

[23] Yongtaek Lee, R. D. Noble, B. Y. Yeomb, Y. I. Park, K. H. Lee, ¨Analysis of CO2 removal by hollow fiber membrane contactors¨, Journal of Membrane Science, 194 (2001), pp 57-67.

[24] George Xomeritakis, Chung-Yi Tsai, C. Jeffrey Brinkera, ¨Microporous sol-gel derived aminosilicate membrane for enhanced carbon dioxide separation¨, Separation and purification technology, 42 (2005), pp 249-257.

[25] S. H. Yeon, K. S. Lee, B. Sea, Y. I. Park, K. H. Lee, ¨Application of pilot-scale membrane contactor hybrid system for removal of carbon dioxide from flue gas¨, Journal of Membrane Science, 257 (2005), pp 156-160

[26] L. Cheng, L. Zhang, H. Chen, C. Gao, ¨Carbon dioxide removal from air by microalgae cultured in a membrane-photobioreactor¨, Separation and Purification Technology, Article in press, 2006.

[27] Kirk and Othmer, ¨Encyclopedia of chemical technology¨, volume 1, fourth edition, pp 493-539.

[28] Ralph T. yang, ¨Adsorbents: fundamentals and application¨, Wiley interscience publication, pp 79-117.

[29] Ralph T. yang, ¨Gas separation by adsorption processes¨, Imperial college press, volume 1, pp 9-44.

[30] Serna-Guerrero R, Belmabkhout Y, Sayari A. Triamine-grafted pore-expanded mesoporous silica for CO¡sub¿2¡/sub¿ capture: Effect of moisture and adsorbent regeneration strategies. Adsorption;16(6):567-575.

[31] Dutta BK. Principles of Mass Transfer and Separation Processes, Prentice Hall of India, New Delhi. 2007.

[32] Yang RT. Gas Separation by Adsorption Processes, Imperial College Press, London, 1997.

[33] Xiao P, Zhang J, Webley P, Li G, Singh R, Todd R. Capture of CO¡sub¿2¡/sub¿ from flue gas streams with zeolite 13X by vacuum-pressure swing adsorption. Adsorption 2008;14(4-5):575-582.

[34] Zhou L, Wu J, Li M, Wu Q, Zhou Y. Prediction of multicomponent adsorption equilibrium of gas mixtures including supercritical components. Chemical Engineering Science 2005;60(11):2833-2844.

[35] Belmabkhout Y, Serna-Guerrero R, Sayari A. Adsorption of CO¡sub¿2¡/sub¿ from dry gases on MCM-41 silica at ambient temperature and high pressure. 1: Pure CO¡sub¿2¡/sub¿ adsorption. Chemical Engineering Science 2009;64(17):3721-3728.

[36] Caskey SR, Wong-Foy AG, Matzger AJ. Dramatic tuning of carbon dioxide uptake via metal substitution in a coordination polymer with cylindrical pores. Journal of the American Chemical Society 2008;130(33):10870-10871.

[37] Li;Y.; Zhao; C.; Chen; H.; Liang; C.; Duan; L.; Zhou W. Modified CaO-based sorbent looping cycle for CO2 mitigation.,. Fuel, 2009;88:697.

[38] Yue; M; Sun L, B.; Cao, Y.; Wang, J.; Wang, Y.; Yu, Q.; Zhu, J. Promoting the CO2 adsorption in the amine-containing SBA-15 by hydroxyl group. Microporous Mesoporous Mater 2008;114:74

[39] Abanades J, C.;. The maximum capture efficiency of CO2 using a carbonation/calcination cycle of CaO/CaCO3.,. Chem Eng J, 2002;90:303.

[40] Pravin D, Jadhav, R. V. Chatti, Rajesh, B. Biniwale, Nitin, K. Labhsetwar, Sadhana, S. Rayalu. Monoethanol amine modified zeolite 13X for CO2 adsoption at diffrent temperatures,. Energy & Fuels, 2007;21:3555-3559.

[41] Chatti R, Bansiwal AK, Thote JA, Kumar V, Jadhav P, Lokhande SK, et al. Amine loaded zeolites for carbon dioxide capture: Amine loading and adsorption studies. Microporous and Mesoporous Materials 2009;121(1-3):84-89.

[42] Xu X, Zhao X, Sun L, Liu X. Adsorption separation of carbon dioxide, methane and nitrogen on monoethanol amine modified [beta]-zeolite. Journal of Natural Gas Chemistry 2009;18(2):167-172.

[43] Plaza MG, Pevida C, Arenillas A, Rubiera F, Pis JJ. CO¡sub¿2¡/sub¿ capture by adsorption with nitrogen enriched carbons. Fuel 2007;86(14 SPEC. ISS.):2204-2212.

[44] Somy A, Mehrnia MR, Amrei HD, Ghanizadeh A, Safari M. Adsorption of carbon dioxide using impregnated activated carbon promoted by Zinc. International Journal of Greenhouse Gas Control 2009;3(3):249-254.

[45] Chen C, Yang ST, Ahn WS, Ryoo R. Amine-impregnated silica monolith with a hierarchical pore structure: Enhancement of CO¡sub¿2¡/sub¿ capture capacity. Chemical Communications 2009(24):3627-3629.

[46] Li P, Ge B, Zhang S, Chen S, Zhang Q, Zhao Y. CO2 capture by polyethylenimine-modified fibrous adsorbent. Langmuir 2008;24(13):6567-6574.

[47] Chang FY, Chao KJ, Cheng HH, Tan CS. Adsorption of CO¡sub¿2¡/sub¿ onto amine-grafted mesoporous silicas. Separation and Purification Technology 2009;70(1):87-95.

[48] Arenillas A. SK, Drage T.C. and Snape C.E. CO2 capture using some fly ash-derived carbon materials. Fuel, 2005;84:2204-2210.

[49] Belmabkhout Y, Serna-Guerrero R, Sayari A. Adsorption of CO¡sup¿2¡/sup¿-containing gas mixtures over amine-bearing pore-expanded MCM-41 silica: Application for gas purification. Industrial and Engineering Chemistry Research;49(1):359-365.

[50] Chang ACC, Chuang SSC, Gray M, Soong Y. In-situ infrared study of CO2 adsorption on SBA-15 grafted with -(aminopropyl)triethoxysilane. Energy and Fuels 2003;17(2):468-473.

[51] Sanz R, Calleja G, Arencibia A, Sanz-Prez ES. CO2 adsorption on branched polyethyleneimine-impregnated mesoporous silica SBA-15. Applied Surface Science;256(17):5323-5328.

[52] Douglas M. Ruthven and Shamsuzzaman farooq, ¨Pressure swing adsorption˝, VCH publishers, pp 1-30.

[53] P. C. Wankat, ¨Rate controlled separations˝, Springer international edition, pp 405-435.

[54] Li P, Zhang S, Chen S, Zhang Q, Pan J, Ge B. Preparation and adsorption properties of polyethylenimine containing fibrous adsorbent for carbon dioxide capture. Journal of Applied Polymer Science 2008;108(6):3851-3858.

# Index